Supporting Information

Molecular design of near-infrared (NIR) fluorescent probes targeting exo-peptidase and application for detection of dipeptidyl peptidase 4 (DPP-4) activity

Yuki Hoshino,[a] Kenjiro Hanaoka,*[,b] Kei Sakamoto,[c] Masahiro Yasunaga,[d] Takashi Kojima,[e] Daisuke Kotani,[e] Ayumu Nomoto,[a] Eita Sasaki,[b] Toru Komatsu,[a] Tasuku Ueno,[a] Hiroyuki Takamaru,[f] Yutaka Saito,[f] Yasuyuki Seto,[b] and Yasuteru Urano*[,a,g]

[a] Graduate School of Pharmaceutical Sciences, [g] Graduate School of Medicine, The University of Tokyo, 7-3-1 Hongo, Bunkyo-ku, Tokyo 113-0033, Japan. [b] Graduate School of Pharmaceutical Sciences, Keio University, 1-5-30 Shibakoen, Minato-ku, Tokyo 105-8512, Japan. [c] Department of Gastrointestinal Surgery, Graduate School of Medicine, The University of Tokyo, 7-3-1 Hongo, Bunkyo-ku, Tokyo 113-8655, Japan. [d] Division of Developmental Therapeutics, Research Center for Innovative Oncology, National Cancer Center Hospital East, 6-5-1 Kashiwanoha, Kashiwa, Chiba 277-8577, Japan. [e] Department of Gastroenterology and Gastrointestinal Oncology, National Cancer Center Hospital East, 6-5-1, Kashiwanoha, Kashiwa-shi, Chiba, 277-8577, Japan. [f] Endoscopy Division, National Cancer Center Hospital, 5-1-1 Tsukiji, Chuo-ku, Tokyo 104-0045, Japan.

*Correspondence and requests for materials should be addressed to Y.U. and K.H. (Y.U., email: uranokun@m.u-tokyo.ac.jp) (K.H., email: khanaoka@keio.jp).

Experimental details

General procedure and materials: Reagents and solvents were of the best grade available, purchased from Tokyo Chemical Industries, Wako Pure Chemical, Sigma-Aldrich, Kanto Chemical Company, Dojindo, Watanabe Chemical Industry, Gibco, Invitrogen and Thermo Scientific, and were used without further purification. Mice (BALB/cAJcl, BALB/cAJcl-*nu-nu*) were purchased from CLEA Japan, Inc. Saline was purchased from Fuso Pharmaceutical Industry, Ltd. Reactions were monitored by means of TLC and ESI mass spectrometry, or by UPLC-MS. All compounds were purified on a silica gel column, or by GPC, reversed-phase MPLC and/or preparative HPLC.

Enzymes and inhibitors: Leucine aminopeptidase, microsomal from porcine kidney (L5006), human recombinant dipeptidyl peptidase 4 (D4943), human recombinant dipeptidyl peptidase 7 (D3321), human recombinant dipeptidyl peptidase 8 (D3196), human recombinant dipeptidyl peptidase 9 (D3071), recombinant prolyl oligopeptidase (O9515), prolidase from porcine kidney (P6675) and human recombinant fibroblast active protein (SRP0294) were purchased from Sigma-Aldrich. Bestatin (58970-76-6) was purchased from Wako Pure Chemical. Sitagliptin phosphate (13252) was purchased from Cayman Chemical Company. K579 (D3572) was purchased from Sigma-Aldrich. Linagliptin (CS0637) was purchased from ChemScene LLC.

Instruments: NMR spectra were recorded on a JEOL ECZ-400S instrument at 400 MHz for ^{1}H NMR and at 100 MHz for ^{13}C NMR. Mass spectra (MS) were measured with a JEOL JMS-T100LC AccuToF (ESI). Column chromatography using silica gel was performed on a MPLC system (Yamazen Smart Flash EPCLC AI-5805 (Tokyo, Japan)). Reversed-phase MPLC purification was performed on an IsoleraTM One (Biotage) equipped with a SNAP Ultra C18 30 g (Biotage). Preparative HPLC was performed on an Inertsil ODS-3 (10.0 × 250 mm) column (GL Sciences Inc.) using an HPLC system composed of a pump (PU-2080, JASCO) and a detector (MD-2015 or FP-2025, JASCO), using eluent A (H_2O containing 0.1% TFA (v/v)) and eluent B (CH_3CN with 20% H_2O containing 0.1% TFA (v/v)) or eluent C ((H_2O containing 100 mM TEAA, i.e., 100 mM triethylamine acetate aqueous solution) and eluent D (CH_3CN with 20% H_2O containing 100 mM TEAA) at the flow rate of 3 or 5

mL/min. HPLC analyses were performed on a system composed of a pump (PU-2080, JASCO) and a detector (MD-2015, JASCO), using eluent A and eluent B at the flow rate of 1 mL/min. GPC purification was performed on a recycle preparative HPLC LC-9110 NEXT (Japan Analytical Industry) equipped with a JAIGEL-2HR column (20 mm × 600 mm, Japan Analytical Industry). Peptide synthesis was performed on a Syro I instrument (Biotage). Absorption spectra were obtained with a Shimadzu UV-1850 (Tokyo, Japan). Fluorescence spectroscopic studies were performed with a Hitachi F7100 (Tokyo, Japan). The slit width was 5 nm for both excitation and emission. The photomultiplier voltage was 700 V. Absolute fluorescence quantum yields were determined with a Hamamatsu Photonics Quantaurus-QY.

Measurement of photophysical properties: Photophysical properties of dyes were examined in PBS (pH = 7.4) containing 0.1% (v/v) DMSO as a co-solvent. The absolute fluorescence quantum yields (Φ_{fi}) were determined with a Hamamatsu Photonics Quantaurus-QY.

Fluorometric assay: Unless otherwise mentioned, the fluorometric assay of enzymes and cell lysates was performed in 10 mM HEPES buffer (pH = 7.4) at 37°C. Disposable cells, quartz cells or flat-bottom 384-well plates (Corning, 4511) were used for the assay. Fluorescence was detected with a fluorometer (Hitachi F7100 (Tokyo, Japan)) or a microplate reader (Perkin Elmer, EnVision 2103 Multilabel Reader).

Kinetic assay: Enzymatic reactions with 1, 5, 10, 25, 50 and 100 μM probes were performed in 20 μL of 10 mM HEPES buffer (pH = 7.4) containing 1% DMSO as a co-solvent using 2.4 ng DPP-4 or 0.22 ng LAP at 37°C. Flat-bottom 384-well plates (Corning, 4511) were used for the assay. Fluorescence was measured with a microplate reader (Perkin Elmer, EnVision 2103 Multilabel Reader). The excitation and emission wavelengths were 620 nm and 685 nm, respectively. Initial velocity, calculated from the change in fluorescence at 685 nm, was plotted against probe concentration, and fitted to a Michaelis-Menten equation.

Cell culture: H226 cells (ATCC) were cultured in RPMI1640 Medium (Roswell Park Memorial Institute 1640 Medium, Gibco) containing 10% fetal bovine serum (Gibco) and 1% penicillin streptomycin (Gibco). A549 cells (RIKEN BRC) and HEK293 cells (ATCC) were cultured in DMEM (Dulbecco's modified Eagle’s medium, Gibco)

containing 10% fetal bovine serum and 1% penicillin streptomycin. The established cell line KYSE270, originated from well-differentiated human esophageal squamous cell carcinoma, was provided by Y. Shimada, Kyoto University, Japan.[1] KYSE270 cells were cultured in a 1-to-1 mixture of Ham's F12 Nutrient Mixture (Gibco) and RPMI1640 Medium containing 2% fetal bovine serum and 1% penicillin streptomycin. All cells were maintained at 37°C under an atmosphere of 5% CO_2 in air.

Fluorescence confocal microscopy with DPP-4 inhibitors: H226 and KYSE270 cells were plated on 35 mm glass-bottomed dishes (Matsunami Glass Ind., Ltd) and cultured for one day with the appropriate media. Cells were washed with 1 mL HBSS and pre-incubated with or without DPP-4 inhibitor (18 μM sitagliptin) in 1 mL HBSS containing 0.2% DMSO as a co-solvent at 37°C under an atmosphere of 5% CO_2 in air for 30 min. Cells were washed with 1 mL HBSS, and then incubated with 1 μM **GP-SiR640**, **EP-SiR640**, **DP-SiR640** or **SP-SiR640** in 1 mL HBSS containing 0.1% DMSO as a co-solvent for up to 60 min. Fluorescence images were captured using a Leica Application Suite Advanced (LAS-AF) instrument with a Leica TCS SP8 and a 63× objective lens. The light source was a HeNe laser. The excitation and emission wavelengths were 633 nm and 660-695 nm, respectively.

Preparation of cultured cell lysate: H226, A549, HEK293 and KYSE270 cells were cultured in 10 cm dishes (Thermo Scientific) with the appropriate media. When the cells reached 70-80% confluency, they were washed with PBS (-) twice, and lysed by addition of 1 mL CelLyticM (Sigma-Aldrich, C2978) to the plate, followed by incubation at room temperature for 15 min. The solution was collected and centrifuged (14,000 rpm × 10 min at 4˚C). The supernatant was collected, aliquoted, and stored at -80˚C. Protein concentration was determined with the standard BCA assay, and the concentrations of the cell lysates were adjusted to 0.5 mg/mL with PBS (-). The diluted lysate was aliquoted for single use, and stored at -80°C.

Fluorescence confocal microscopy with various cells: H226, KYSE270, A549 and HEK293 cells were plated on 35 mm glass-bottomed dishes (Matsunami Glass Ind., Ltd) and cultured for one day with the appropriate media. Cells were washed with 1 mL HBSS and then incubated with 1 μM **EP-SiR640** in 1 mL HBSS containing 0.1% DMSO as a co-solvent for 10 min. Fluorescence images were captured using LAS-AF instrument with a Leica TCS

SP8 and a 63× objective lens. The light source was a HeNe laser. The excitation and emission wavelengths were 633 nm and 660-695 nm, respectively.

***In vivo* imaging of mice**: All procedures were approved by the Animal Care and Use Committee of the University of Tokyo. BALB/cAJcl mice (male, 6 weeks old) were purchased from CLEA Japan, Inc. Mice were orally administered with saline or the DPP-4 inhibitor (10 mg/kg/day sitagliptin in saline, or 1 mg/kg/day linagliptin in saline) for 1 week. Then the mice were anesthetized with isoflurane, the abdominal cavities were exposed, and 100 μM **EP-SiR640** in 100 μL saline containing 1% DMSO as a co-solvent was injected via the tail vein. Fluorescence images were captured with a Maestro^{TM} In-Vivo Imaging System (PerkinElmer, Inc., MA, USA) equipped with an excitation filter set at 635 nm (616-661 nm) and a 675 nm emission long-path filter. Fluorescence images at 700 nm were extracted and the fluorescence intensity was quantified by ImageJ software.

***Ex vivo* imaging of mice**: All procedures were approved by the Animal Care and Use Committee of the University of Tokyo. BALB/cAJcl mice (male, 6 weeks old) were purchased from CLEA Japan, Inc. Mice were orally administered with saline or the DPP-4 inhibitor (0.1, 1 or 10 mg/kg/day sitagliptin in saline, or 0.01, 0.1, 1 mg/kg/day linagliptin in saline) for 3 days. Then the mice were anesthetized with isoflurane, and sacrificed by cervical dislocation. The organs (kidneys, spleen, liver, heart, lung, stomach, intestines, caecum) were extracted and washed with saline twice. All organs were incubated with 10 μM **EP-SiR640** in 1.5 mL saline containing 0.1% DMSO as a co-solvent for 20 min. Fluorescence images were captured with a Maestro^{TM} In-Vivo Imaging System (PerkinElmer, Inc., MA, USA) equipped with an excitation filter set at 635 nm (616-661 nm) and a 675 nm emission long-path filter. Fluorescence images at 700 nm were extracted and the fluorescence intensity was quantified by ImageJ software.

***In vivo* imaging of tumor-bearing mice**: All procedures were approved by the Animal Care and Use Committee of the University of Tokyo. BALB/cAJcl-*nu*-*nu* mice (female, 5 weeks old) were purchased from CLEA Japan, Inc. 1.0×10^7 H226 cells suspended in a 1-to-1 mixture of PBS (pH = 7.4) and Matrigel (Corning, 356234) were injected into the left flank 3-4 weeks before imaging. For imaging, the mice were anesthetized with isoflurane and

intratumorally administered with saline or DPP-4 inhibitor (0.05 mg sitagliptin in 10 μL saline). After 20 min, the mice were intratumorally injected with 100 μM **EP-SiR640** in 10 μL saline. Fluorescence images were captured with a Maestro™ In-Vivo Imaging System (PerkinElmer, Inc., MA, USA) equipped with an excitation filter set at 635 nm (616-661 nm) and a 675 nm emission long-path filter. Fluorescence images at 700 nm were extracted and the fluorescence intensity was quantified by ImageJ software.

Fluorescence imaging of sections of biopsy tumors and normal tissues from esophageal cancer patients: The experimental protocols and procedures were approved (No. 2018-064) by the institutional review board of the National Cancer Center, Japan. All methods were performed in accordance with the relevant guidelines and regulations. Tumors and normal tissues from esophageal cancer patients were resected, and stored at -80°C. Each specimen was sliced to 10 μm with a cryostat (LEICA CM1860), mounted on a slide glass, air-dried, and stored again at -80°C. Each sample was incubated with 1 μM **EP-SiR640** and DAPI (Invitrogen) in 1 mL HBSS containing 0.1% DMSO as a co-solvent for 50 min. Fluorescence images were captured with a KEYENCE Fluorescence Microscope BZ-X. The excitation and emission wavelengths were 620/60 and 700/75 nm for **EP-SiR640**, and 360/40 and 460/50 nm for DAPI, respectively. Resected specimens were evaluated pathologically with hematoxylin and eosin (H&E) staining to confirm the presence of tumor.

Fluorescence imaging of esophageal cancer in ESD clinical specimens: All experiments were performed in accordance with guidelines and regulations approved by the Research Ethics Committee of the University of Tokyo and registered in the UMIN Clinical Trials Registry (registration number: UMIN000012645). All methods were performed in accordance with the relevant guidelines and regulations. Specimens from esophageal cancer patients were resected during ESD. 50 μM **EP-SiR640** in PBS (pH = 7.4) containing 0.5% DMSO as a co-solvent was applied to each specimen. Fluorescence images were captured with a Maestro™ In-Vivo Imaging System (PerkinElmer, Inc., MA, USA) equipped with an excitation filter set at 635 nm (616-661 nm) and a 675 nm emission long-path filter. Fluorescence images at 700 nm were extracted.

Fluorescence imaging of esophageal cancer in clinical specimens resected by ESD: The experimental protocols

and procedures were approved (No. 2014-370) by the institutional review board of the National Cancer Center, Japan. All methods were performed in accordance with the relevant guidelines and regulations. Specimens from esophageal cancer patients were resected by means of ESD. Each specimen was sprayed with 50 μM **EP-SiR640** in PBS (pH = 7.4) containing 0.5% DMSO as a co-solvent. Fluorescence images were captured with a Discovery™ imaging system (INDEC, Inc., CA, USA) equipped with Deep Red filter set (Cy5 filter set, Ex = 630 nm, Em = 670 nm).

Computation details: All density functional theory (DFT) calculations were performed at the B3LYP[2–5] functional level as implemented in Gaussian 09[6]. The 6-31+G(d) basis set was used for all atoms. The number of imaginary frequencies is 0 for all structures.

Synthesis and characterization of compounds

Scheme 1. Synthesis of 2,6-diMe SiR640 and Ac-2,6-diMe SiR640.

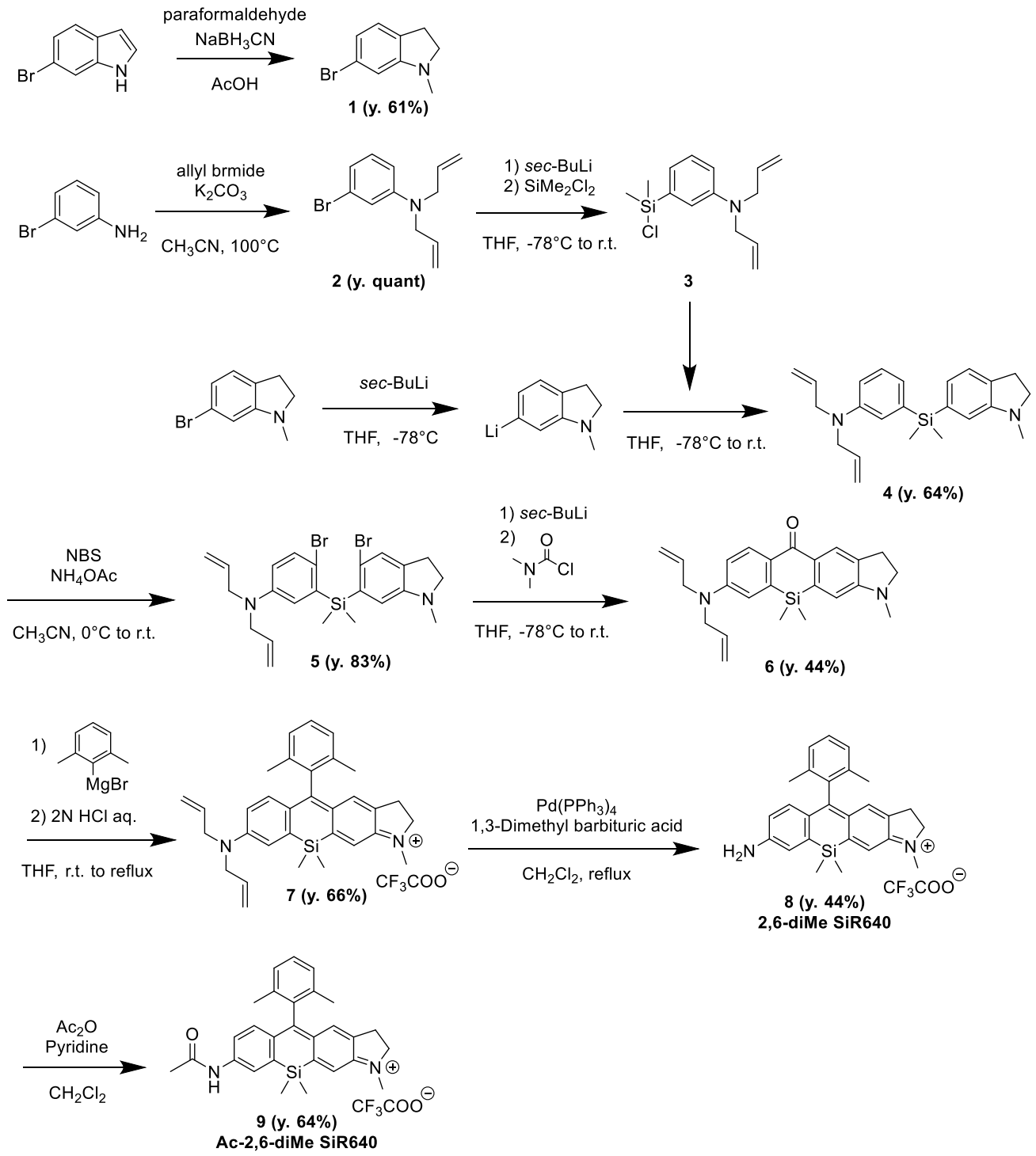

6-Bromo-1-methylindoline

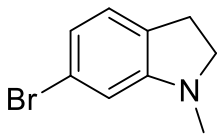

1

The compound was synthesized according to the literature.[7]

3-Bromo-*N*,*N*-diallylaniline

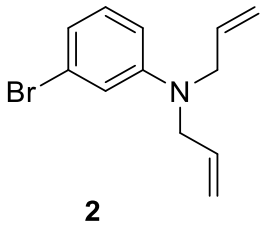

2

The compound was synthesized according to the literature.[8]

***N*,*N*-Diallyl-3-[dimethyl(1-methylindolin-6-yl)silyl]aniline**

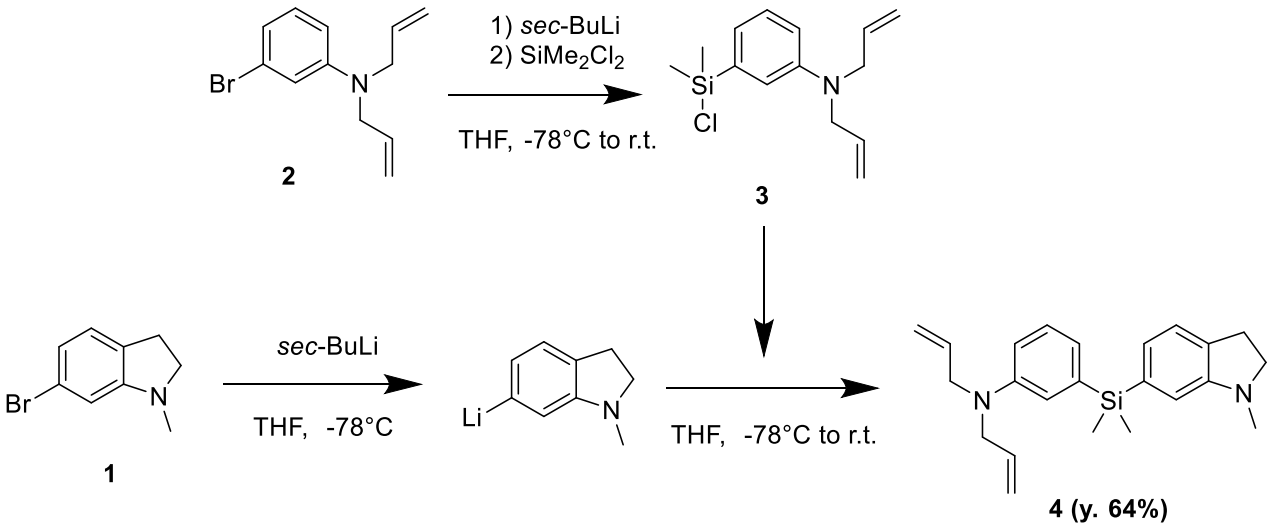

2 **3** **1** **4 (y. 64%)**

To a 100 mL well-dried flask flushed with argon, a solution of **2** (655 mg, 2.60 mmol) in 20 mL anhydrous THF

was added. The solution was cooled to -78°C, and *sec*-BuLi (2.6 mL, 1.0 M, 2.6 mmol) was added under an argon atmosphere. The mixture was stirred at the same temperature for 15 min, then dichlorodimethylsilane (3.1 mL, 26 mmol) in 2 mL anhydrous THF was added at -78°C. The reaction mixture was warmed to room temperature and stirred for 1 h. The solvent and the excess dichlorodimethylsilane were removed by evaporation, and compound **3** was dried *in vacuo* for 1 h. To a 100 mL well-dried flask flushed with argon, **1** (551 mg, 2.60 mmol) in 10 mL anhydrous THF was added. The solution was cooled to -78°C, and *sec*-BuLi (2.6 mL, 1.0 M, 2.6 mmol) was added. The mixture was stirred at the same temperature for 15 min, then a solution of **3** in 5 mL anhydrous THF was added at -78°C. The reaction mixture was warmed to room temperature and stirred for 1 h. The reaction was quenched with H_2O and the aqueous layer was extracted with CH_2Cl_2. The combined organic layers were washed with brine, dried over Na_2SO_4 and evaporated to dryness. The residue was purified by column chromatography (silica gel, AcOEt/*n*-hexane) to give pure **4** (604 mg, 1.67 mmol, 64% yield). ^{1}H-NMR (400 MHz, $CDCl_3$): δ 0.53 (s, 6H), 2.76 (s, 3H), 2.95 (t, *J* = 8.2Hz, 2H), 3.29 (t, *J* = 8.2Hz, 2H), 3.91-3.92 (m, 4H), 5.13-5.20 (m, 4H), 5.81-5.90 (m, 2H), 6.67 (s, 1H), 6.72 (dd, *J* = 2.7, 8.2 Hz, 1H), 6.87-6.92 (m, 3H), 7.10 (d, *J* = 6.9Hz, 1H), 7.21 (t, *J* = 8.2Hz, 1H); ^{13}C-NMR (100 MHz, $CDCl_3$): δ -1.98, 28.9, 36.4, 53.0, 56.1, 112.4, 113.3, 116.2, 118.3, 122.4, 124.0, 124.4, 128.6, 131.7, 134.3, 137.1, 139.2, 148.0, 152.9; HRMS (ESI$^+$): Calcd for 363.2257 $[M + H]^+$; Found, 363.2214 (-4.3 mDa).

***N,N*-Diallyl-4-bromo-3-[(5-bromo-1-methylindolin-6-yl)dimethylsilyl]aniline**

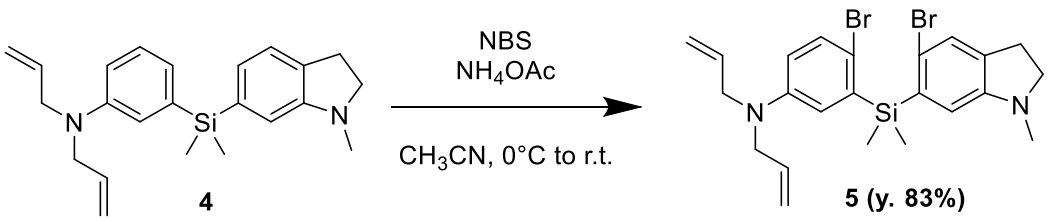

To a solution of **4** (1.76 g, 4.85 mmol) in 20 mL CH_3CN, NH_4OAc (74.8 mg, 0.971 mmol) was added. The solution was cooled to 0°C, then NBS (*N*-bromosuccinimide) (1.73 g, 9.71 mmol) was added. The mixture was

stirred for 30 min at 0°C, then warmed to room temperature, stirred for 2 h, and diluted with sat. $NaHCO_3$ aq. The aqueous layer was extracted with CH_2Cl_2. The combined organic layers were washed with brine, dried over Na_2SO_4 and evaporated to dryness. The residue was purified by column chromatography (silica gel, AcOEt/*n*-hexane) to give pure **5** (2.09 g, 4.02 mmol, 83% yield). ^{1}H-NMR (400 MHz, CD_3CN): δ 0.64 (s. 6H), 2.64 (s, 3H), 2.86 (t, *J* = 8.2Hz, 2H), 3.24 (t, *J* = 8.2Hz, 2H), 3.82-3.83 (m, 4H), 4.98-5.07 (m, 4H), 5.71-5.81 (m, 2H), 6.53-6.56 (m, 2H), 6.75 (d, *J* = 3.7Hz, 1H), 7.15 (s, 1H), 7.21 (d, *J* = 8.7Hz, 1H); ^{13}C-NMR (100 MHz, CD_3CN): δ -1.46, 28.0, 35.2, 53.0, 55.7, 114.8, 115.1, 115.2, 115.5, 117.1, 121.6, 128.6, 132.8, 134.1, 134.9, 136.4, 138.7, 147.0, 152.5; HRMS (ESI^+): Calcd for 519.0467 $[M + H]^+$; Found, 519.0485 (+1.8 mDa).

8-(Diallylamino)-1,10,10-trimethyl-2,3-dihydro-5H-benzo[5,6]silino[3,2-f]indol-5-one

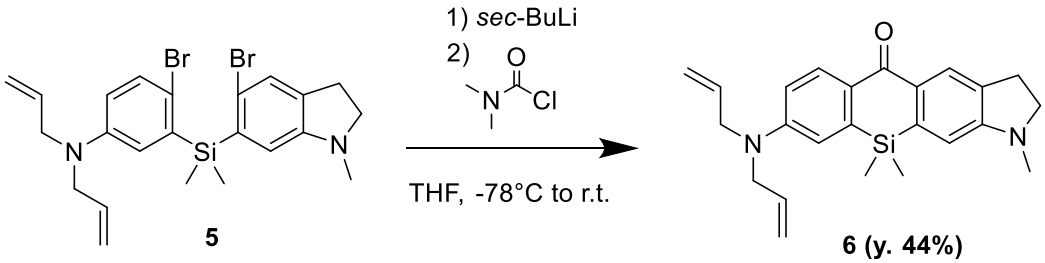

To a 100 mL well-dried flask flushed with argon, a solution of **5** (1.08 g, 2.08 mmol) in 30 mL THF was added. The solution was cooled to -78°C, and *sec*-BuLi (4.0 mL, 1.0 M, 4.0 mmol) was added under an argon atmosphere. The reaction mixture was stirred at the same temperature for 15 min, then a solution of dimethylcarbamoyl chloride (95.5 μL, 1.04 mmol) in 2 mL anhydrous THF was added at -78°C. The reaction mixture was warmed to room temperature and stirred for 30 min. The reaction was quenched with sat. NH_4Cl aq. and the aqueous layer was extracted with AcOEt. The combined organic layers were washed with brine, dried over Na_2SO_4 and evaporated to dryness. The residue was purified by column chromatography (silica gel, AcOEt/*n*-hexane) to give pure **6** (359 mg, 0.924 mmol, 45% yield). ^{1}H-NMR (400 MHz, $CDCl_3$): δ 0.41 (s. 6H), 2.89 (s, 3H), 3.04 (t, *J* = 8.2Hz, 2H), 3.46 (t, *J* = 8.2Hz, 2H), 4.01-4.02 (m, 4H), 5.17-5.21 (m, 4H), 5.82-5.91 (m, 2H), 6.48 (s, 1H), 6.78-6.82 (m, 2H), 8.19 (s, 1H), 8.33 (d, *J* = 8.7Hz, 1H); ^{13}C-NMR (100 MHz, $CDCl_3$): δ -1.05, 28.1, 34.7, 52.7, 54.9, 108.0, 113.5, 114.7,

116.6, 126.1, 130.0, 131.6, 131.7, 132.2, 133.1, 140.2, 140.4, 150.1, 154.9, 185.2; HRMS (ESI^+): Calcd for 389.2049 $[M + H]^+$; Found, 389.2033 (-1.6 mDa).

***N,N*-Diallyl-2,6-diMe SiR640 (7)**

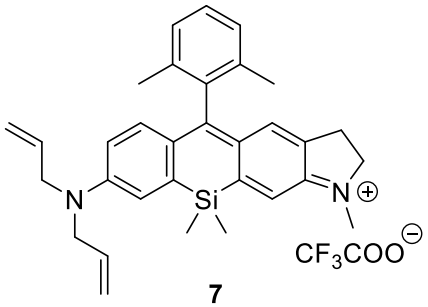

7

The compound was synthesized according to the literature.[9]

2,6-diMe SiR640 (8)

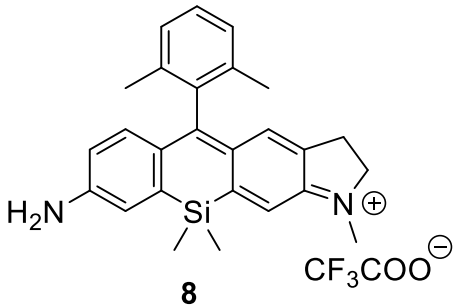

8

2,6-diMe SiR640

The compound was synthesized according to the literature.[9]

Ac-2,6-diMe SiR640 (9)

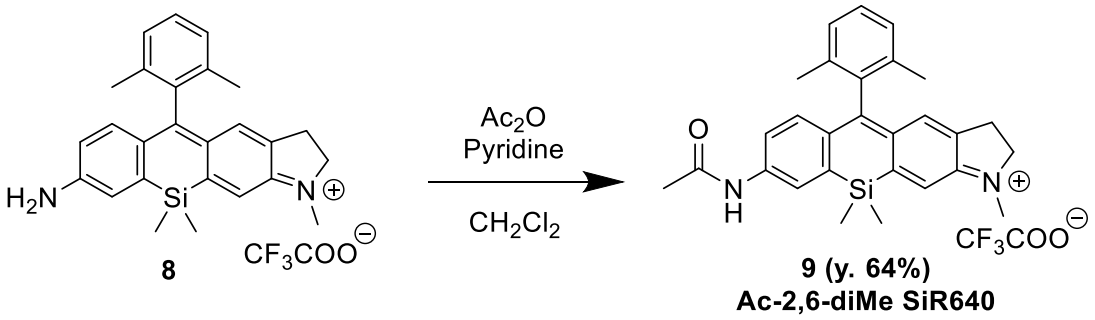

To the solution of **8** (6.6 mg, 12.9 μmol) in 5 mL CH_2Cl_2, acetic anhydride (157 μL, 1.67 mmol) and pyridine (134 μL, 1.67 mmol) were added. The mixture was stirred at r.t. for 24 h, then evaporated to dryness. The residue was taken up in H_2O and extracted with CH_2Cl_2. The combined organic layers were washed with brine, dried over Na_2SO_4 and evaporated to dryness. The residue was purified by HPLC (eluent: A: H_2O, 0.1% TFA (v/v), B: CH_3CN/H_2O = 80/20, 0.1% TFA (v/v); gradient: A/B = 80/20 to 0/100, 25 min) to give **Ac-2,6-diMe SiR640** (**9**) (4.6 mg, 8.32 μmol, 64% yield). ^{1}H-NMR (400 MHz, CD_3OD): δ 0.58 (s. 6H), 1.96 (s, 6H), 2.14 (s, 3H), 3.01 (t, *J* = 6.4 Hz, 2H), 3.51 (s, 3H), 4.09 (t, *J* = 6.4 Hz, 2H), 6.85 (s, 1H), 6.96 (d, *J* = 9.2 Hz, 1H), 7.23 (d, *J* = 7.3 Hz, 2H), 7.35 (t, *J* = 7.3 Hz, 1H), 7.49 (dd, *J* = 2.3, 9.2 Hz, 1H), 7.57 (s, 1H), 8.12 (d, *J* = 2.3 Hz, 1H); HRMS (ESI$^+$): Calcd for 439.2206 $[M]^+$; Found, 439.2192 (-1.4 mDa). The HPLC chromatogram after purification is shown below (eluent: A: H_2O, 0.1% TFA (v/v), B: CH_3CN/H_2O = 80/20 0.1% TFA (v/v); gradient: A/B = 80/20 to 0/100, 25 min; flow rate: 1.0 mL/min; detection: absorbance at 500 nm).

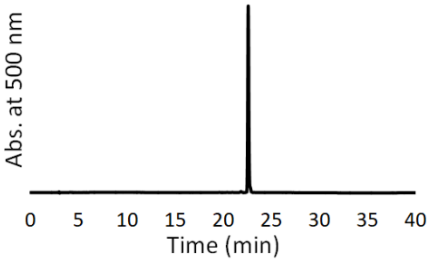

Scheme 2. Synthesis of 2,6-diMe JuloSiR and Ac-2,6-diMe JuloSiR.

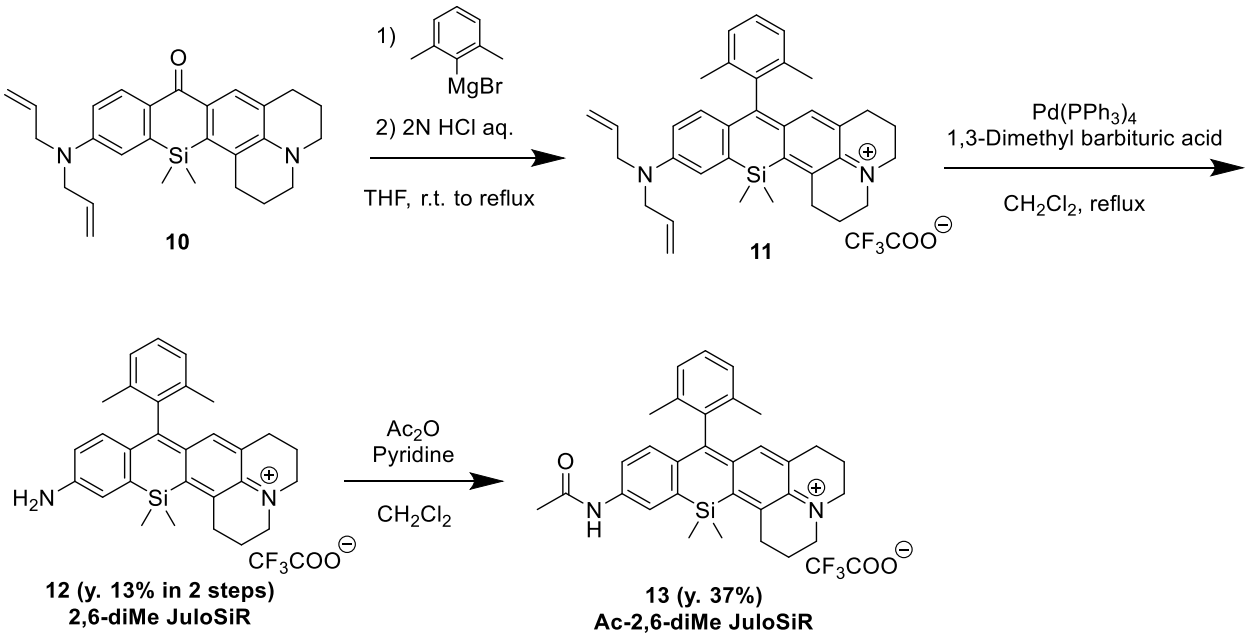

12-(Diallylamino)-14,14-dimethyl-1,2,3,5,6,7-hexahydro-1H,9H-benzo[5,6]silino[2,3-f]pyrido-[3,2,1-ij]quinoli n-9-one

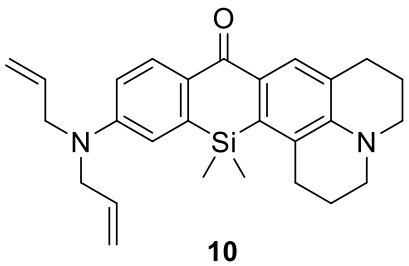

10

The compound was synthesized according to the literature.[10]

2,6-diMe JuloSiR (12)

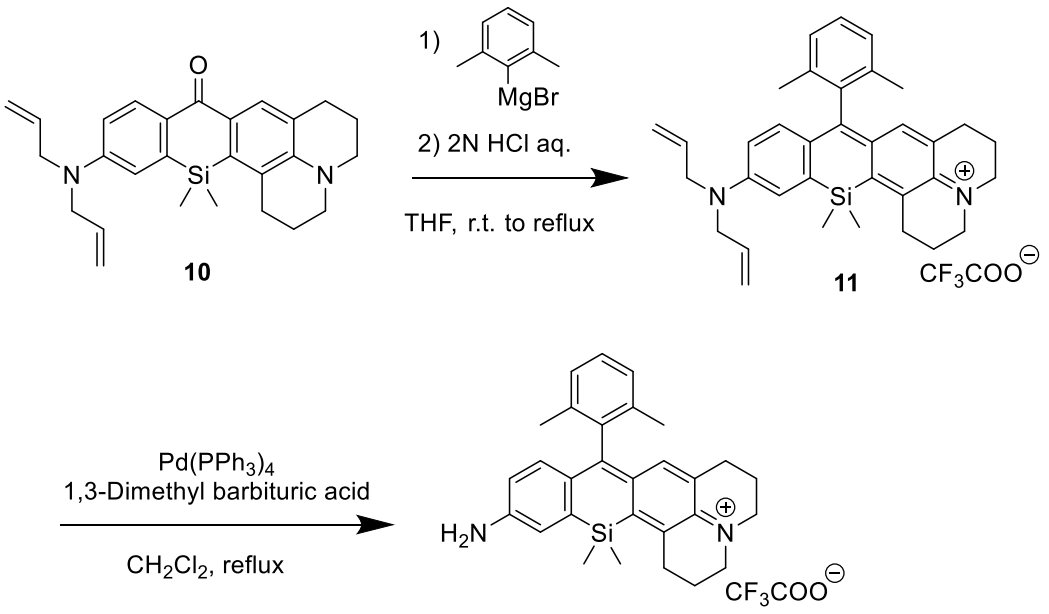

12 (y. 13% in 2 steps)
2,6-diMe JuloSiR

To a 50 mL well-dried flask flushed with argon, a solution of **10** (60 mg, 0.140 mmol) in 15 mL anhydrous THF was added. Then, THF solution of 2,6-dimethylphenylmagnesium bromide (1.4 mL, 1.0 M, 1.4 mmol) was added and the mixture was refluxed at 85°C for 3 h under an argon atmosphere. Another portion of Grignard reagent was further added two times (1.0 M THF solution of 2,6-dimethylphenylmagnesium bromide; 1.4 mL, 1.4 mmol at 3 h and 2.8 mL, 2.8 mmol at 7 h after the first Grignard reagent was added) and the mixture was refluxed at 85°C for 6 h. It was allowed to cool to room temperature, and 2N HCl aq. was added. The reaction mixture was diluted with H_2O, and the aqueous layer was extracted with CH_2Cl_2. The combined organic layers were washed with brine, dried over Na_2SO_4 and evaporated to dryness. The residue was purified with reversed-phase MPLC (CH_3CN, 0.1% TFA (v/v) /H_2O, 0.1% TFA (v/v)). Then, the compound was lyophilized. The residue (crude **11**) was dissolved in 8 mL deoxidized CH_2Cl_2, and 1,3-dimethylbarbituric acid (28.5 mg, 0.182 mmol) and $Pd(PPh_3)_4$ (28.5 mg, 60.5 μmol) were added. The reaction mixture was refluxed at 40°C for 16.5 h under an argon atmosphere, then cooled to room temperature, and diluted with H_2O. The aqueous layer was extracted with CH_2Cl_2. The combined organic layers were washed with brine, dried over Na_2SO_4 and evaporated to dryness. The residue was purified by HPLC (eluent:

A: H_2O, 0.1% TFA (v/v), B: CH_3CN/H_2O = 80/20, 0.1% TFA (v/v); gradient: A/B = 70/30 to 0/100, 25 min), and the partially purified compound was lyophilized. The residue was further purified by HPLC (eluent: C: H_2O, 100 mM TEAA, D: CH_3CN/H_2O (100 mM TEAA) = 80/20; gradient: C/D = 70/30 to 0/100, 25 min), and again lyophilized. The residue was further purified by HPLC (eluent: A: H_2O, 0.1% TFA (v/v), B: CH_3CN/H_2O = 80/20, 0.1% TFA (v/v); gradient: A/B = 70/30 to 0/100, 30 min) to give **2,6-diMe JuloSiR** (**12**) (9.8 mg, 17.8 μmol, 13% yield). ^{1}H-NMR (400 MHz, CD_3OD): δ 0.60 (s, 6H), 1.86-1.98 (m, 8H), 2.05-2.11 (m, 2H), 2.46 (t, *J* = 6.0 Hz, 2H), 3.02 (t, *J* = 6.0 Hz, 2H), 3.56-3.62 (m, 4H), 6.48 (dd, *J* = 2.3, 9.2 Hz, 1H), 6.75 (s, 1H), 6.80 (d, *J* = 9.2 Hz, 1H), 7.10 (d, *J* = 2.3 Hz, 1H), 7.18 (d, *J* = 7.8 Hz,, 2H), 7.31 (t, *J* = 7. 8 Hz, 1H); ^{13}C-NMR (100 MHz, CD_3OD): δ -2.32, 18.4, 20.2, 20.6, 27.1, 28.7, 51.2, 51.9, 115.4, 121.6, 124.7, 126.5, 126.6, 127.2, 128.3, 133.2, 135.4, 138.1, 138.8, 139.1, 141.8, 147.5, 151.4, 155.8, 167.7; HRMS (ESI$^+$): Calcd for 437.2413 $[M]^+$; Found, 437.2395 (-1.8 mDa).

Ac-2,6-diMe JuloSiR (13)

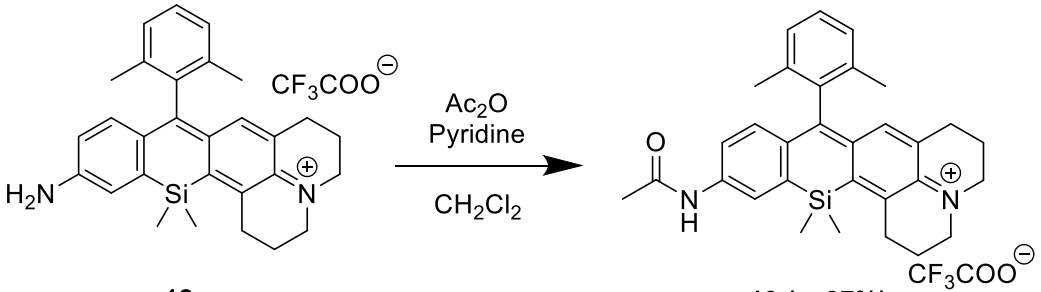

12 **13 (y. 37%)**
Ac-2,6-diMe JuloSiR

To a solution of **12** (5.7 mg, 10.4 μmol) in 5 mL CH_2Cl_2, acetic anhydride (123 μL, 1.30 mmol) and pyridine (105 μL, 1.30 mmol) were added. The mixture was stirred at r.t. for 21 h, then evaporated to dryness and H_2O was added to the residue. The aqueous layer was extracted with CH_2Cl_2. The combined organic layers were washed with brine, dried over Na_2SO_4 and evaporated to dryness. The residue was purified by HPLC (eluent: A: H_2O, 0.1% TFA (v/v), B: CH_3CN/H_2O = 80/20, 0.1% TFA (v/v); gradient: A/B = 80/20 to 0/100, 25 min) to give pure **Ac-2,6-diMe JuloSiR** (**13**) (2.3 mg, 3.88 μmol, 37% yield). ^{1}H-NMR (400 MHz, CD_3OD): δ 0.65 (s, 6H), 1.94-1.99 (m, 8H),

2.10-2.18 (m, 5H), 2.52 (t, *J* = 6.0 Hz, 2H), 3.09 (t, *J* = 6.0 Hz, 2H), 3.74-3.79 (m, 4H), 4.95, 6.89-6.91 (m, 2H), 7.22 (d, *J* = 7.8 Hz, 2H), 7.35 (t, *J* = 7.8 Hz, 1H) 7.47 (dd, *J* = 2.3, 9.2 Hz, 1H), 8.13 (d, *J* = 2.3 Hz, 1H); HRMS (ESI^+): Calcd for 479.2519 $[M]^+$; Found, 479.2479 (-4.0 mDa). The HPLC chromatogram after purification is shown below (eluent: A: H_2O, 0.1% TFA (v/v), B: CH_3CN/H_2O = 80/20, 0.1% TFA (v/v); gradient: A/B = 80/20 to 0/100, 25 min; flow rate: 1.0 mL/min; detection: absorbance at 500 nm).

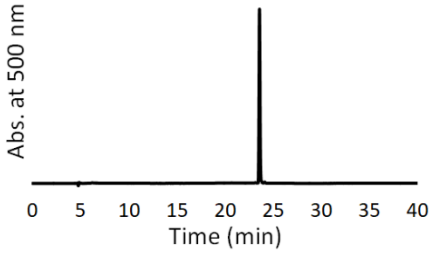

Scheme 3. Synthesis of 2,6-diMe QuinoSiR and Ac-2,6-diMe QuinoSiR.

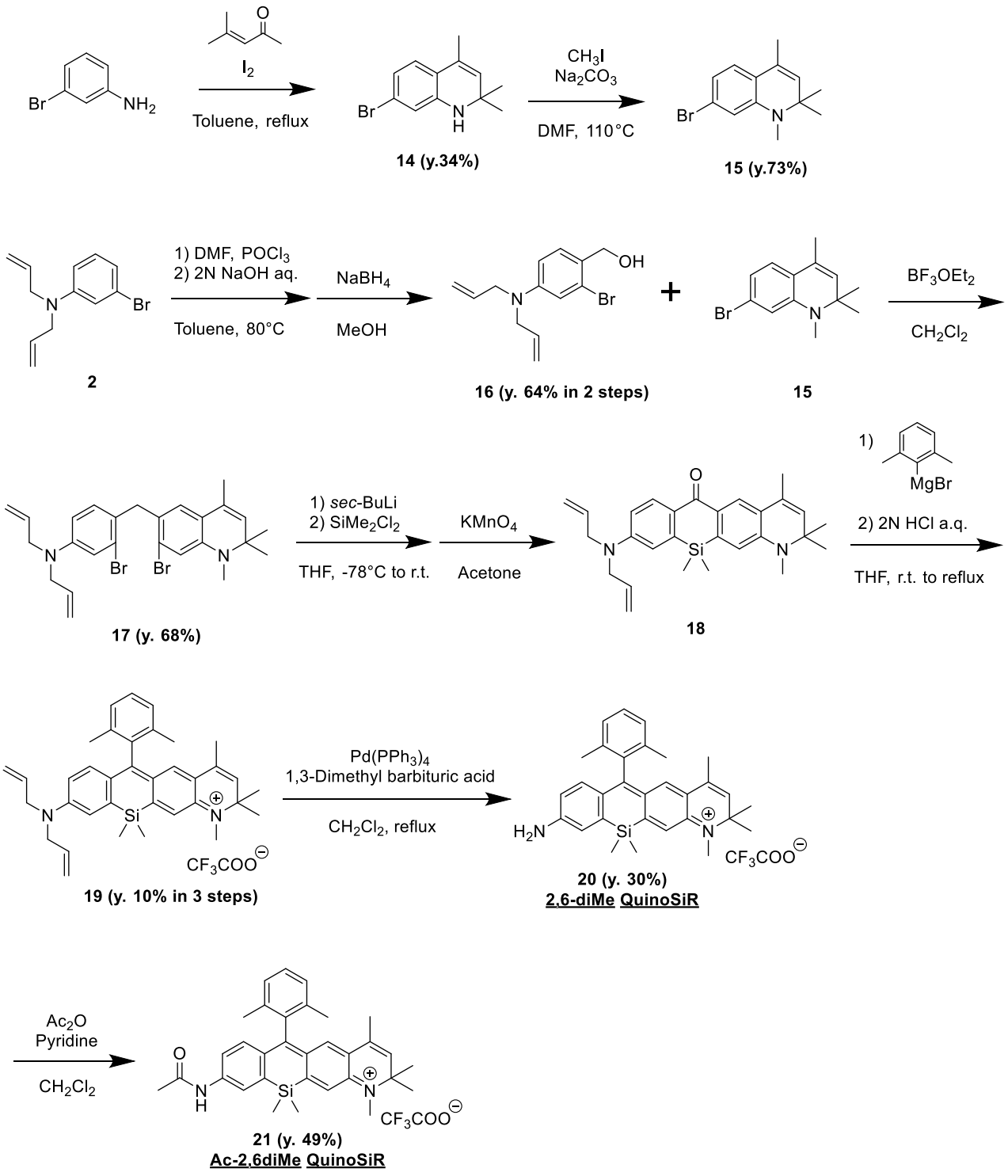

7-Bromo-2,2,4-trimethyl-1,2-dihydroquinoline

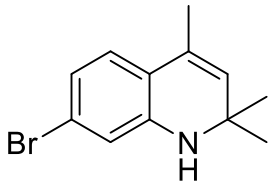

14

The compound was synthesized according to the literature.[7]

7-Bromo-1,2,2,4-tetramethyl-1,2-dihydroquinoline

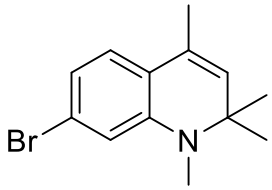

15

The compound was synthesized according to the literature.[7]

2-Bromo-4-(diallylamino)phenyl]methanol

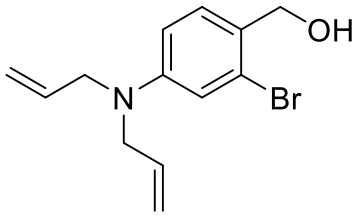

16

The compound was synthesized according to the literature.[9]

***N*,*N*-Diallyl-3-bromo-4-[(7-bromo-1,2,2,4-tetramethyl-1,2-dihydroquinolin-6-yl)methyl]aniline**

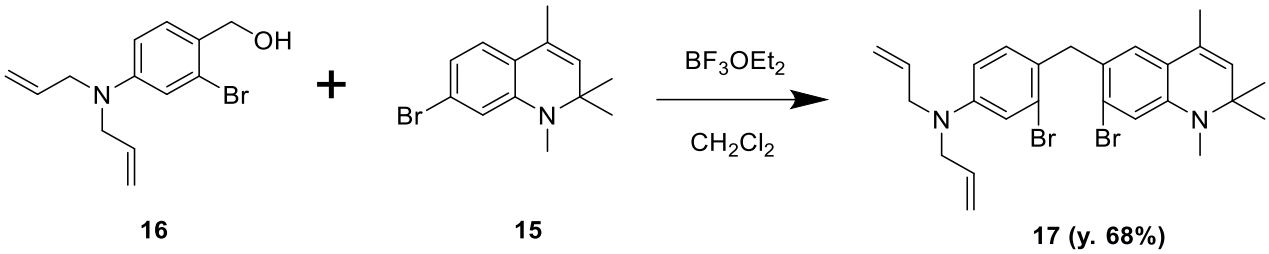

16 **15** **17 (y. 68%)**

To a solution of **16** (2.14 g, 7.57 mmol) and **15** (2.02 g, 7.57 mmol) in 100 mL CH_2Cl_2, $BF_3{\cdot}OEt_2$ (1.90 mL, 15.1 mmol) was added and the mixture was stirred at r.t. for 21 h. The reaction mixture was diluted with H_2O and the aqueous layer was extracted with CH_2Cl_2. The combined organic layers were washed with brine, dried over Na_2SO_4 and evaporated to dryness. The residue was purified by column chromatography (silica gel, AcOEt/*n*-hexane) to give **17** (2.72 g, 5.13 mmol, 68% yield). ^{1}H-NMR (400MHz, $CDCl_3$): δ 1.28 (s, 6H), 1.85 (d, *J* = 1.4Hz, 3H), 2.76 (s, 3H), 3.85-3.86 (m, 4H), 3.96 (s, 2H), 5.12-5.17 (m, 4H), 5.28 (d, *J* = 1.4Hz, 1H), 5.76-5.86 (m, 2H), 6.51 (dd, *J* = 2.7, 8.7Hz, 1H), 6.69 (s, 1H), 6.74-6.77 (m, 2H), 6.90 (d, *J* = 2.7Hz, 1H); ^{13}C-NMR (100 MHz, $CDCl_3$): δ 18.5, 27.3, 30.8, 40.0, 52.9, 56.5, 111.7, 114.4, 116.0, 116.3, 122.9, 124.9, 125.4, 125.7, 126.5, 127.1, 127.7, 130.4, 130.6, 133.6, 144.8, 148.1; HRMS (ESI$^+$): Calcd for 529.0854 $[M + H]^+$; Found, 529.0859 (+0.5 mDa).

***N,N*-Diallyl-2,6-diMe QuinoSiR (19)**

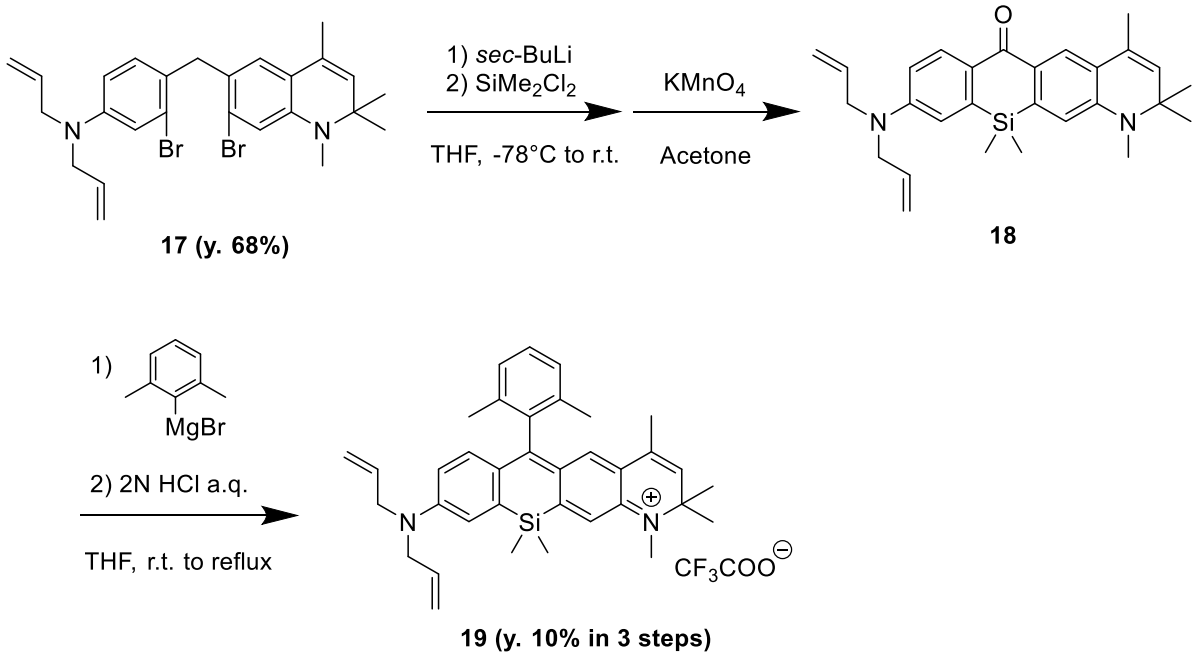

To a 50 mL well-dried flask flushed with argon, a solution of **17** (542 mg, 1.02 mmol) in 12 mL anhydrous THF was added. The solution was cooled to -78°C, and *sec*-BuLi (2.1 mL, 1.0 M, 2.1 mmol) was added under an argon atmosphere. The reaction mixture was stirred at the same temperature for 15 min, then dichlorodimethylsilane (244 μL, 2.04 mmol) in 3 mL anhydrous THF was added. The reaction mixture was warmed to room temperature and stirred for 2 h. The reaction was quenched with water and the aqueous layer was extracted with CH_2Cl_2. The combined organic layers were washed with brine, dried over Na_2SO_4 and evaporated to dryness. The residue was dissolved in 30 mL acetone and the solution was cooled to 0°C. $KMnO_4$ (646 mg, 4.09 mmol) was added in small portions over 2 h with stirring at the same temperature. Stirring was continued at the same temperature for 1 h, then the mixture was diluted with CH_2Cl_2, and filtered through a Celite filter. The filtrate was evaporated to dryness. The residue was purified by column chromatography (silica gel, AcOEt/*n*-hexane) and GPC to afford crude **18**, which was dissolved in 10 mL anhydrous THF. To this solution was added a THF solution of 2,6-dimethylphenylmagnesium bromide (2.2 mL, 1.0 M, 2.2 mmol), and the mixture was refluxed at 85°C for 2 h under an argon atmosphere. Another portion of Grignard reagent (1.0 M THF solution of

2,6-dimethylphenylmagnesium bromide; 2.2 mL, 2.2 mmol) was further added and the mixture was refluxed at 85°C for 5 h. It was then cooled to room temperature, and 2 N HCl aq. was added. The resulting mixture was diluted with H_2O, and the aqueous layer was extracted with CH_2Cl_2. The combined organic layers were washed with brine, dried over Na_2SO_4 and evaporated to dryness. The residue was purified by reversed-phase MPLC (CH_3CN, 0.1% TFA (v/v) /H_2O, 0.1% TFA (v/v)), and the product was lyophilized. The resulting partially purified compound was further purified by HPLC (eluent: A: H_2O, 0.1% TFA (v/v), B: CH_3CN/H_2O = 80/20, 0.1% TFA (v/v); gradient: A/B = 60/40 to 0/100, 15 min) to give ***N,N*-diallyl-2,6-diMe QuinoSiR** (**19**) (68.6 mg, 0.106 mmol, 10% in 3 steps). ^{1}H-NMR (400 MHz, CD_3CN): δ 0.53 (s, 6H), 1.43 (s, 6H), 1.47 (d, *J* = 1.4 Hz, 3H), 1.94 (s, 6H), 3.27 (s, 3H), 4.17-4.18 (m, 4H), 5.15-5.23 (m, 4H), 5.50-5.51 (m, 1H), 5.83-5.92 (m, 2H), 6.64-6.67 (m, 2H), 6.98 (d, *J* = 9.6 Hz, 1H), 7.19-7.22 (m, 4H), 7.33 (t, *J* = 7.3 Hz, 1H); ^{13}C-NMR (100 MHz, CD_3CN): δ –2.24, 16.6, 18.9, 28.0, 33.2, 53.1, 61.0, 114.5, 117.0, 120.9, 121.0, 123.4, 125.4, 127.2, 127.3, 127.5, 128.6, 131.1, 131.2, 131.9, 135.5, 138.4, 138.9, 146.4, 151.5, 151.6, 153.0, 168.4; HRMS (ESI$^+$): Calcd for 531.3196 $[M]^+$; Found, 531.3189 (-0.7 mDa).

2,6-diMe QuinoSiR (20)

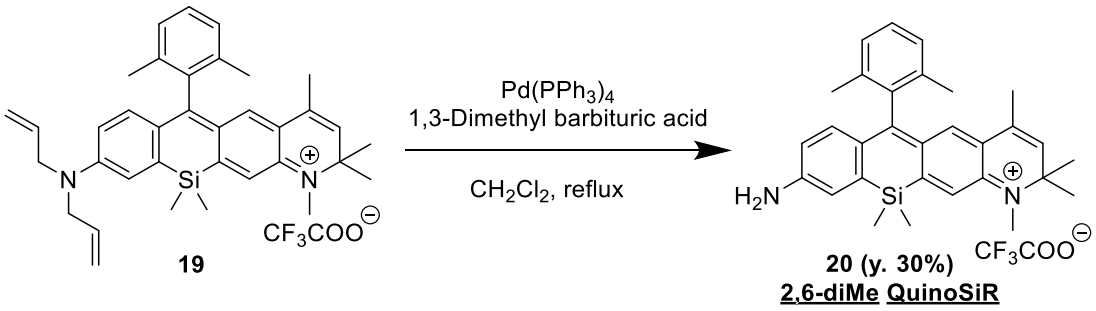

To a solution of **19** (68.6 mg, 0.106 mmol) in 15 mL deoxidized CH_2Cl_2, 1,3-dimethylbarbituric acid (61.5 mg, 0.394 mmol) and $Pd(PPh_3)_4$ (151 mg, 0.138 mmol) were added. The reaction mixture was refluxed at 40°C for 21 h under an argon atmosphere, then cooled to room temperature, and diluted with H_2O. The aqueous layer was extracted with CH_2Cl_2. The combined organic layers were washed with brine, dried over Na_2SO_4 and evaporated to

dryness. The residue was purified by reversed-phase MPLC (CH_3CN, 0.1% TFA (v/v) /H_2O, 0.1% TFA (v/v)). The product was lyophilized and further purified by HPLC (eluent: A: H_2O, 0.1% TFA (v/v), B: CH_3CN/H_2O = 80/20, 0.1% TFA (v/v); gradient, A/B = 70/30 to 0/100, 25 min) to give **2,6-diMe QuinoSiR** (**20**) (17.9 mg, 31.7 μmol, 30% yield). ^{1}H-NMR (400 MHz, CD_3CN): δ 0.51 (s, 6H), 1.43 (s, 6H), 1.47 (s, 3H), 1.94 (s, 6H), 3.26 (s, 3H), 5.49 (s, 1H), 6.58 (d, *J* = 9.2 Hz, 1H), 6.66 (s, 1H), 6.97 (d, *J* = 9.2 Hz, 1H), 7.17-7.22 (m, 4H), 7.32 (t, *J* = 7.3 Hz, 1H); ^{13}C-NMR (100 MHz, CD_3CN): δ -0.24, 16.6, 18.8, 28.0, 33.1, 61.0, 116.0, 120.9, 122.9, 123.3, 125.4, 127.0, 127.4, 127.5, 128.6, 131.1, 131.2, 135.5, 138.4, 140.1, 147.6, 151.2, 151.5, 155.6, 169.0; HRMS (ESI$^+$): Calcd for 451.2570 $[M]^+$; Found, 451.2570 (+0.0 mDa).

Ac-2,6-diMe QuinoSiR (21)

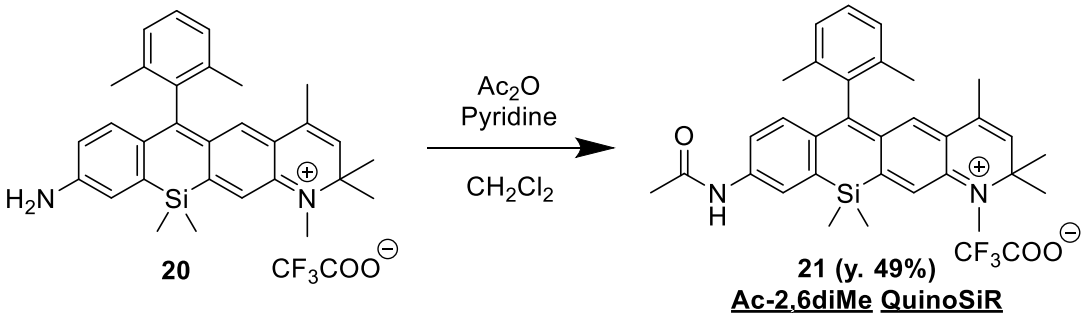

To a solution of **20** (8.0 mg, 14.2 μmol) in 5 mL CH_2Cl_2, acetic anhydride (134 μL, 1.42 mmol) and pyridine (114 μL, 1.42 mmol) were added and the mixture was stirred at r.t. for 14 h. The reaction mixture was evaporated to dryness and H_2O was added to the residue. The aqueous layer was extracted with CH_2Cl_2. The combined organic layers were washed with brine, dried over Na_2SO_4 and evaporated to dryness. The residue was purified by HPLC (eluent: A: H_2O, 0.1% TFA (v/v), B: CH_3CN/H_2O = 80/20, 0.1% TFA (v/v); gradient: A/B = 80/20 to 0/100, 25 min) to give **Ac-2,6-diMe QuinoSiR** (**21**) (4.2 mg, 6.92 μmol, 49% yield). ^{1}H-NMR (400 MHz, CD_3OD): δ 0.60 (s, 6H), 1.56-1.57 (m, 9H), 1.97 (s, 6H), 2.16 (s, 3H), 3.59 (s, 3H), 5.78 (s, 1H), 6.82 (s, 1H), 7.07 (d, *J* = 8.7 Hz, 1H), 7.26 (d, *J* = 7.3 Hz, 2H), 7.38 (t, *J* = 7.3 Hz, 1H), 7.53-7.56 (m, 2H), 8.15 (d, *J* = 2.3, 1H); HRMS (ESI$^+$): Calcd for 493.2675 $[M]^+$; Found, 493.2657 (-1.8 mDa). The HPLC chromatogram after purification is shown below (eluent:

A: H_2O, 0.1% TFA (v/v), B: CH_3CN/H_2O = 80/20, 0.1% TFA (v/v); gradient: A/B = 80/20 to 0/100, 25 min; flow rate: 1.0 mL/min; detection: absorbance at 550 nm).

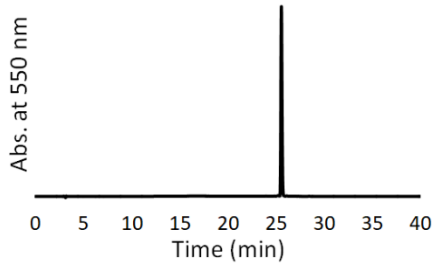

General procedure for peptide synthesis (compounds 22-24)

All peptides were synthesized by the standard Fmoc solid-phase method, using 2-chlorotrityl chloride resin (1.47 mmol/g, 100-200 mesh, 1% DVB). Details are as follows. Coupling cycles: 4 equivalents of Fmoc-amino acid or Boc-amino acid and 4 equivalents of HATU were dissolved in DMF and 8 equivalents of DIEA was added to the mixture. The solution was added to the resin bearing *N*-deprotected peptides, and the resin was shaken for 40 min. Fmoc deprotection cycles: Fmoc deprotection was performed by adding 40% piperidine (v/v) in DMF to the resin and shaking for 12 min. Cleavage: Cleavage of peptides from the resin was done by shaking the resin in the mixture of 20% HFIP (v/v) in CH_2Cl_2 for 30 min. The resin was removed by filtration and the combined filtrate with toluene as an azeotropic agent was evaporated to dryness.

Boc-Glu(O*t*Bu)-Pro-OH (22)

HRMS (ESI$^-$): Calcd for 399.2131 [M - H]$^-$; Found, 399.2113 (-1.8 mDa).

Boc-Asp(O*t*Bu)-Pro-OH (23)

HRMS (ESI$^-$): Calcd for 385.1975 [M - H]$^-$; Found, 385.1979 (+0.4 mDa).

Boc-Ser(O*t*Bu)-Pro-OH (24)

HRMS (ESI$^-$): Calcd for 357.2026 [M - H]$^-$; Found, 357.2029 (+0.3 mDa).

General procedure for synthesis of compounds 25-29

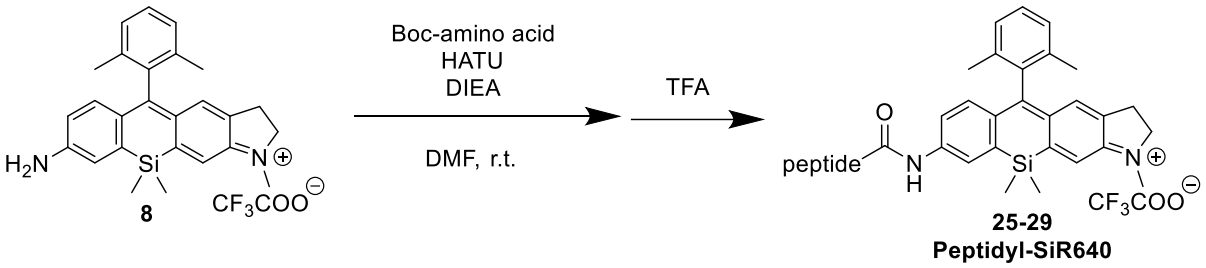

Boc-Gly-Pro-OH and Boc-Leu-OH were purchased from Watanabe Chemical Industry and used without further purification. Other Boc-amino acids were prepared by the standard Fmoc solid-phase method as described above. To a solution of **8** (1 eq.) in DMF, Boc-amino acid (7~9 eq.), HATU (6~8 eq.) and DIEA (12~15 eq.) were added. The mixture was stirred at r.t. overnight, then evaporated to dryness and H_2O was added to the residue. The aqueous layer was extracted with CH_2Cl_2. The combined organic layers were washed with brine, dried over Na_2SO_4 and evaporated to dryness. The residue was dissolved in 1.5 mL TFA and the solution was stirred at r.t. for 30 min, then evaporated to dryness. The resulting product was purified by HPLC (eluent: A: H_2O, 0.1% TFA (v/v), B: CH_3CN/H_2O = 80/20, 0.1% TFA (v/v); gradient: A/B = 80/20 to 0/100, 25 min) to give pure compounds (**25-29**).

Leu-SiR640 (25)

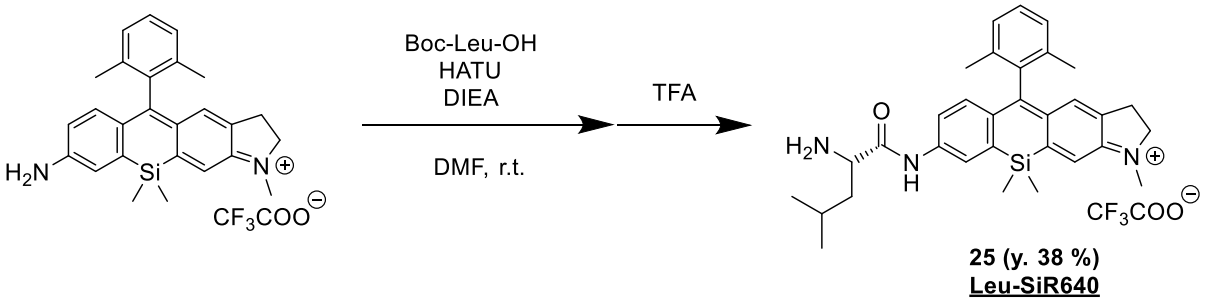

To a solution of **8** (8.1 mg, 15.9 μmol) in 10 mL DMF, Boc-Leu-OH (34.5 mg, 0.139 mmol), HATU (46.5 mg, 0.122 mmol) and DIEA (39.8 μL, 0.234 mmol) were added and the mixture was stirred at r.t. for 18.5 h. The reaction mixture was evaporated to dryness and H_2O was added to it. The aqueous layer was extracted with CH_2Cl_2. The combined organic layers were washed with brine, dried over Na_2SO_4 and evaporated to dryness. The residue was dissolved in 1.5 mL TFA and the solution was stirred at r.t. for 30 min. The reaction mixture was evaporated to dryness and the residue was purified by HPLC (eluent: A: H_2O, 0.1% TFA (v/v), B: CH_3CN/H_2O = 80/20, 0.1% TFA (v/v); gradient: A/B = 80/20 to 0/100, 25 min) to give **Leu-SiR640** (**25**) (3.8 mg, 6.09 μmol, 38% yield). ^{1}H-NMR (400 MHz, CD_3OD): δ 0.59 (s, 6H), 1.01 (d, *J* = 6.0 Hz, 6H), 1.68-1.84 (m, 3H), 1.96 (s, 6H), 3.02 (t, *J* = 6.4 Hz, 2H), 3.53 (s, 3H), 4.04 (t, *J* = 7.3 Hz, 1H), 4.11 (t, *J* = 6.4 Hz, 2H), 6.86 (s, 1H), 7.00 (d, *J* = 9.2 Hz, 1H), 7.24 (d, *J* = 7.3 Hz, 2H), 7.36 (t, *J* = 7.3 Hz, 1H), 7.60-7.63 (m, 2H), 8.13 (d, *J* = 2.3 Hz, 1H); HRMS (ESI$^+$): Calcd for 510.2941 $[M]^+$; Found, 510.2929 (-1.2 mDa). The HPLC chromatogram after purification is shown below (eluent: A: H_2O, 0.1% TFA (v/v), B: CH_3CN/H_2O = 80/20, 0.1% TFA (v/v); gradient: A/B = 80/20 to 0/100, 25 min; flow rate: 1.0 mL/min; detection: absorbance at 500 nm).

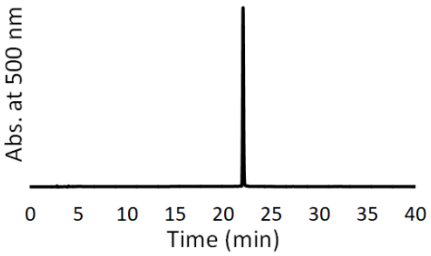

Gly-Pro-SiR640 (26)

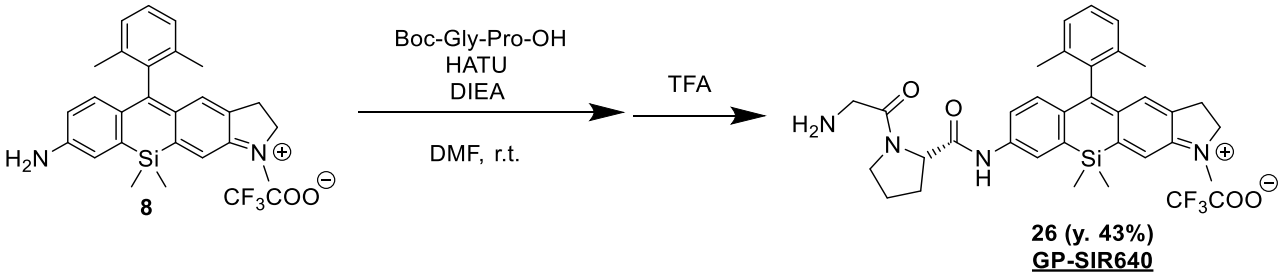

To a solution of **8** (7.4 mg, 14.5 μmol) in 10 mL DMF, Boc-Gly-Pro-OH (34.4 mg, 0.127 mmol), HATU (42.5 mg, 0.112 mmol) and DIEA (36.4 μL, 0.214 mmol) were added and the mixture was stirred at r.t. for 21 h. The reaction mixture was evaporated to dryness and H_2O was added to it. The aqueous layer was extracted with CH_2Cl_2. The combined organic layers were washed with brine, dried over Na_2SO_4 and evaporated to dryness. The residue was dissolved in 1.5 mL TFA and the solution was stirred at r.t. for 30 min, then evaporated to dryness, and the residue was purified by HPLC (eluent: A: H_2O, 0.1% TFA (v/v), B: CH_3CN/H_2O = 80/20, 0.1% TFA (v/v); gradient: A/B = 80/20 to 0/100, 25 min) to give **Gly-Pro-SiR640** (**26**) (4.1 mg, 6.17 μmol, 43% yield). ^{1}H-NMR (400 MHz, CD_3OD): δ 0.58 (d. *J* = 2.7 Hz 6H), 1.91-2.18 (m, 9H), 2.25-2.36 (m, 1H), 3.02 (t, *J* = 6.4 Hz, 2H), 3.52-3.69 (m, 5H), 3.90 (s, 2H), 4.10 (t, *J* = 6.4 Hz, 2H), 4.57-4.60 (m, 1H), 6.85 (s, 1H), 6.97 (d, *J* = 9.2 Hz, 1H), 7.24 (d, *J* = 7.8 Hz, 2H), 7.36 (t, *J* = 7.8 Hz, 1H), 7.52 (dd, *J* = 2.3, 9.2 Hz, 1H), 7.59 (s, 1H), 8.13 (d, *J* = 2.3 Hz, 1H); HRMS (ESI$^+$): Calcd for 551.2842 $[M]^+$; Found, 551.2796 (-4.6 mDa). The HPLC chromatogram after purification is shown below (eluent: A: H_2O, 0.1% TFA (v/v), B: CH_3CN/H_2O = 80/20, 0.1% TFA (v/v); gradient: A/B = 80/20 to 0/100, 25 min; flow rate: 1.0 mL/min; detection: absorbance at 500 nm).

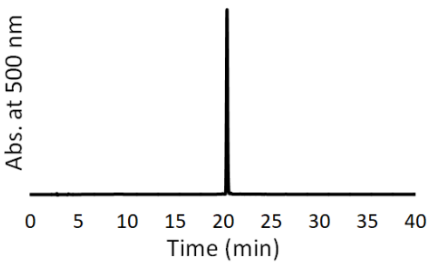

Glu-Pro-SiR640 (27)

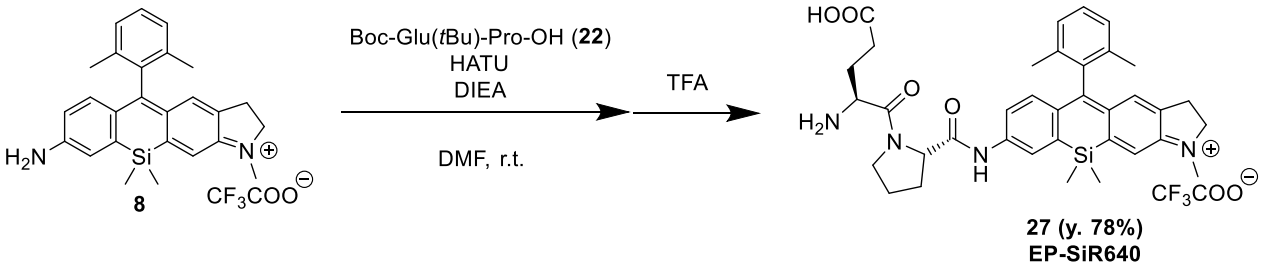

To a solution of **8** (6.4 mg, 12.5 μmol) in 8 mL DMF, Boc-Glu(O*t*Bu)-Pro-OH (34 mg, 85.2 μmol), HATU (28.6 mg, 75.2 μmol) and DIEA (24.5 μL, 0.144 mmol) were added and the mixture was stirred at r.t. for 21 h. The reaction mixture was evaporated to dryness and H_2O was added to it. The aqueous layer was extracted with CH_2Cl_2. The combined organic layers were washed with brine, dried over Na_2SO_4 and evaporated to dryness. The residue was dissolved in 1.5 mL TFA and the solution was stirred at r.t. for 30 min, then evaporated to dryness. The residue was purified by HPLC (eluent: A: H_2O, 0.1% TFA (v/v), B: CH_3CN/H_2O = 80/20, 0.1% TFA (v/v); gradient: A/B = 80/20 to 0/100, 25 min) to give **Glu-Pro-SiR640** (**27**) (7.2 mg, 9.77 μmol, 78% yield). ^{1}H-NMR (400 MHz, CD_3OD): δ 0.58 (d. *J* = 2.3 Hz 6H), 1.91-2.26 (m, 11H), 2.30-2.39 (m, 1H), 2.61 (t, *J* = 7.3 Hz, 2H) , 3.01 (t, *J* = 6.4 Hz, 2H), 3.52 (s, 3H), 3.69-3.79 (m, 2H), 4.10 (t, *J* = 6.4 Hz, 2H), 4.36-4.39 (m, 1H), 4.58-4.62 (m, 1H), 6.85 (s, 1H), 6.97 (d, *J* = 9.2 Hz, 1H), 7.23 (d, *J* = 7.8 Hz, 2H), 7.36 (t, *J* = 7.8 Hz, 1H), 7.50 (dd, *J* = 2.3, 9.2 Hz, 1H), 7.59 (s, 1H), 8.15 (d, *J* = 2.3 Hz, 1H); HRMS (ESI$^+$): Calcd for 623.3054 $[M]^+$; Found, 623.3045 (-0.9 mDa). The HPLC chromatogram after purification is shown below (eluent: A: H_2O, 0.1% TFA (v/v), B: CH_3CN/H_2O = 80/20, 0.1% TFA (v/v); gradient: A/B = 80/20 to 0/100, 25 min; flow rate: 1.0 mL/min; detection: absorbance at 500 nm).

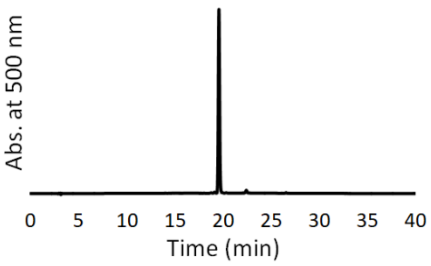

Asp-Pro-SiR640 (28)

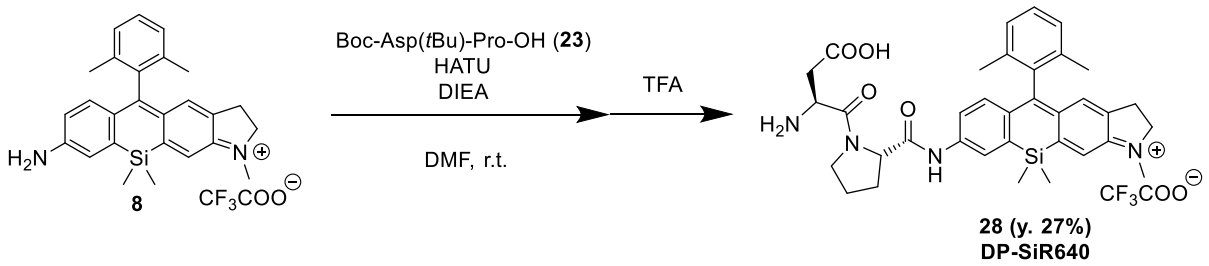

To a solution of **8** (9.3 mg, 18.2 μmol) in 12 mL DMF, Boc-Asp(O*t*Bu)-Pro-OH (61.4 mg, 0.159 mmol), HATU (53.3 mg, 0.140 mmol) and DIEA (46.0 μL, 0.269 mmol) were added and the mixture was stirred at r.t. for 19 h. The reaction mixture was evaporated to dryness and H_2O was added to it. The aqueous layer was extracted with CH_2Cl_2. The combined organic layers were washed with brine, dried over Na_2SO_4 and evaporated to dryness. The residue was dissolved in 1.5 mL TFA and the solution was stirred at r.t. for 30 min, then evaporated to dryness. The residue was purified by HPLC (eluent: A: H_2O, 0.1% TFA (v/v), B: CH_3CN/H_2O = 80/20, 0.1% TFA (v/v); gradient: A/B = 80/20 to 0/100, 25 min) to give **Asp-Pro-SiR640** (**28**) (3.5 mg, 4.84 μmol, 27% yield). ^{1}H-NMR (400 MHz, CD_3OD): δ 0.58 (s, 6H), 1.91-2.17 (m, 9H), 2.29-2.38 (m, 1H), 2.74-2.80 (m, 1H), 3.00-3.11 (m, 3H), 3.52 (s, 3H), 3.64-3.77 (m, 2H), 4.10 (t, *J* = 6.4 Hz, 2H), 4.53-4.56 (m, 1H), 4.59-4.62 (m, 1H), 6.85 (s, 1H), 6.97 (d, *J* = 9.2 Hz, 1H), 7.24 (d, *J* = 7.8 Hz, 2H), 7.36 (t, *J* = 7.8 Hz, 1H), 7.50 (dd, *J* = 2.3, 9.2 Hz, 1H), 7.59 (s, 1H), 8.13 (d, *J* = 2.3 Hz, 1H); HRMS (ESI$^+$): Calcd for 609.2897 $[M]^+$; Found, 609.2891 (-0.6 mDa). The HPLC chromatogram after purification is shown below (eluent: A: H_2O, 0.1% TFA (v/v), B: CH_3CN/H_2O = 80/20, 0.1% TFA (v/v); gradient: A/B = 80/20 to 0/100, 25 min; flow rate: 1.0 mL/min; detection: absorbance at 500 nm).

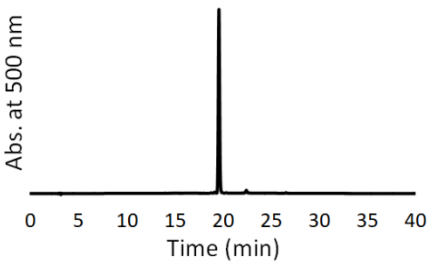

Ser-Pro-SiR640 (29)

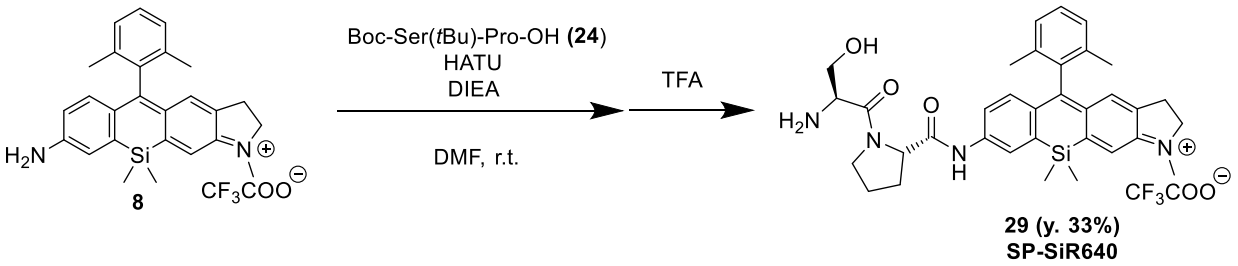

To a solution of **8** (8.8 mg, 17.2 μmol) in 12 mL DMF, Boc-Ser(*t*Bu)-Pro-OH (53.9 mg, 0.150 mmol), HATU (50.5 mg, 0.133 mmol) and DIEA (43.0 μL, 0.255 mmol) were added and the mixture was stirred at r.t. for 19 h. The reaction mixture was evaporated to dryness and H_2O was added to it. The aqueous layer was extracted with CH_2Cl_2. The combined organic layers were washed with brine, dried over Na_2SO_4 and evaporated to dryness. The residue was dissolved in 1.5 mL TFA and the solution was stirred at r.t. for 30 min, then evaporated to dryness. The residue was purified by HPLC (eluent: A: H_2O, 0.1% TFA (v/v), B: CH_3CN/H_2O = 80/20, 0.1% TFA (v/v); gradient: A/B = 80/20 to 0/100 for 25 min) to give **Ser-Pro-SiR640** (**29**) (4.0 mg, 5.76 μmol, 33% yield). ^{1}H-NMR (400 MHz, CD_3OD): δ 0.58 (d, *J* = 1.4 Hz, 6H), 1.91-2.17 (m, 9H), 2.29-2.39 (m, 1H), 3.02 (t, *J* = 6.4 Hz, 2H), 3.52 (s, 3H), 3.66-3.82 (m, 3H), 3.99-4.03 (m, 1H). 4.10 (t, *J* = 6.4 Hz, 2H), 4.28-4.31 (m, 1H),4.59-4.63 (m, 1H), 6.85 (s, 1H), 6.97 (d, *J* = 9.2 Hz, 1H), 7.23 (d, *J* = 7.3 Hz, 2H), 7.36 (t, *J* = 7.3 Hz, 1H), 7.49 (dd, *J* = 2.3, 9.2 Hz, 1H), 7.59 (s, 1H), 8.13 (d, *J* = 2.3 Hz, 1H); HRMS (ESI$^+$): Calcd for 581.2948 $[M]^+$; Found, 581.2950 (+0.2 mDa). The HPLC chromatogram after purification is shown below (eluent: A: H_2O, 0.1% TFA (v/v), B: CH_3CN/H_2O = 80/20, 0.1% TFA (v/v); gradient: A/B = 80/20 to 0/100, 25 min; flow rate: 1.0 mL/min; detection: absorbance at 500 nm).

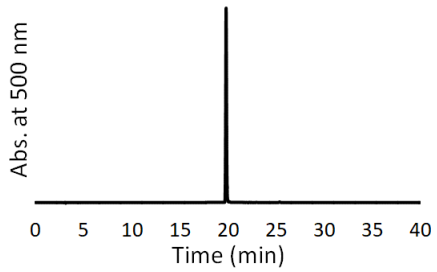

Supporting Figures

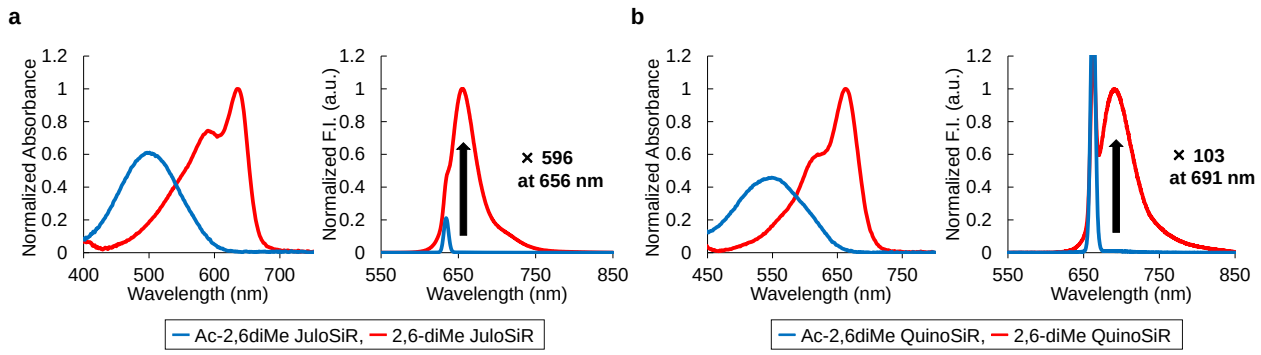

Figure S1. Normalized absorption and emission spectra of 1 μM (a) **2,6-diMe JuloSiR** and **Ac-2,6-diMe JuloSiR** and (b) **2,6-diMe QuinoSiR** and **Ac-2,6-diMe QuinoSiR** in PBS (pH = 7.4) containing 0.1% DMSO as a co-solvent. The excitation wavelengths were 635 nm for (a) and 663 nm for (b). A sharp fluorescence peaks in (a) and (b) are the Rayleigh scattering of the excitation light.

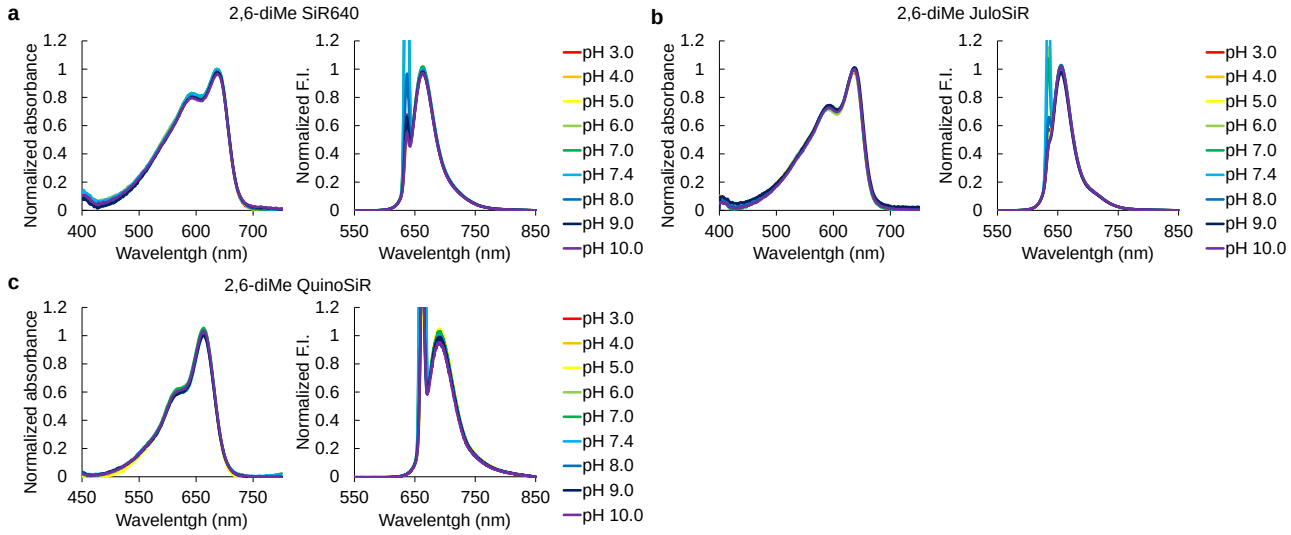

Figure S2. Normalized absorption and emission spectra of 1 μM **2,6-diMe SiR640**, **2,6-diMe JuloSiR** and **2,6-diMe QuinoSiR** in 100 mM NaPi buffer at various pH values. The absorbance and the fluorescence intensity in 100 mM NaPi buffer (pH = 7.4) containing 0.1% DMSO as a co-solvent were set to 1.0 for normalization. The excitation wavelengths were 637 nm for (a), 635 nm for (b), and 663 nm for (c), respectively. A sharp fluorescence

peaks in (a)-(c) are the Rayleigh scattering of the excitation light.

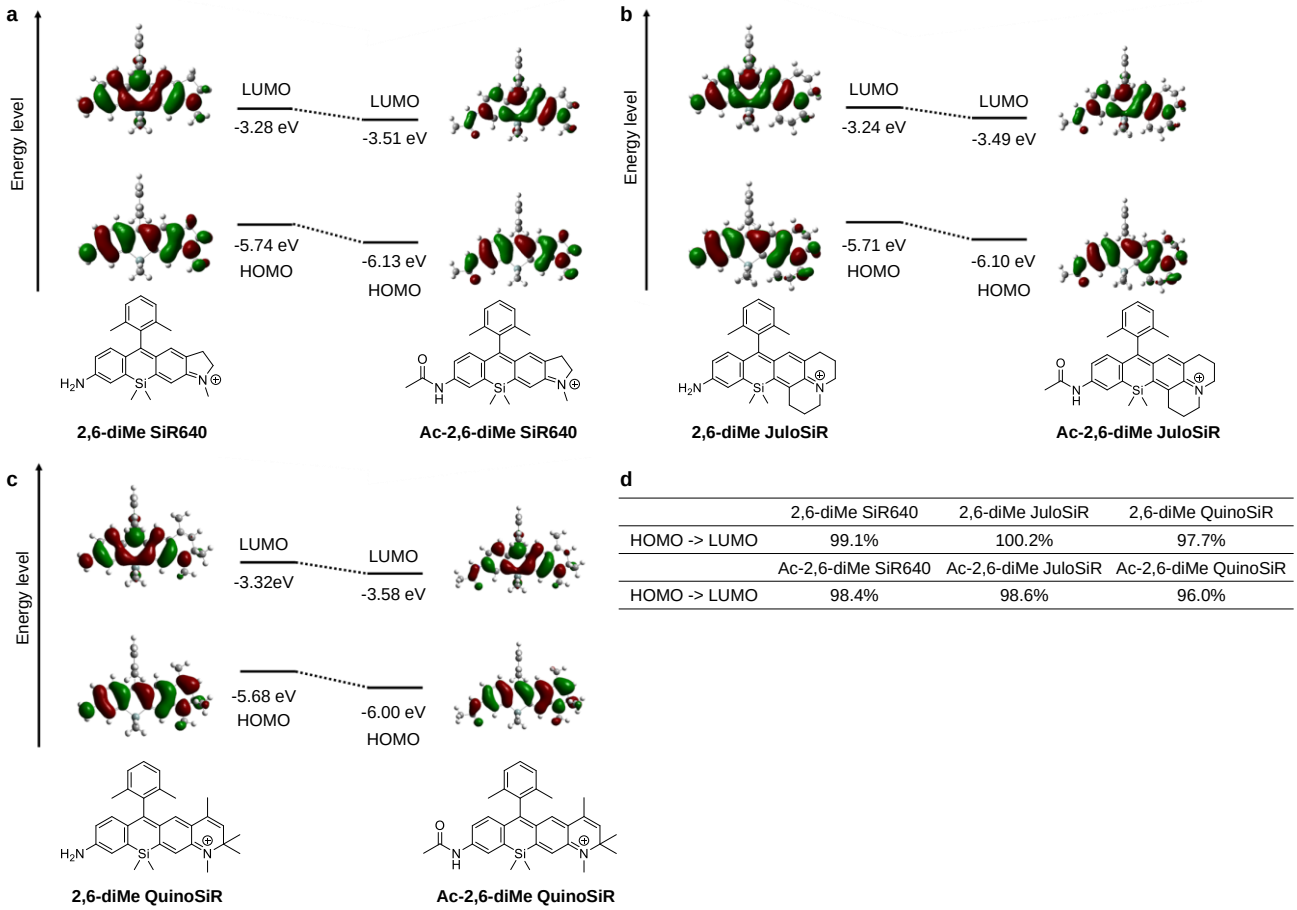

d

	2,6-diMe SiR640	2,6-diMe JuloSiR	2,6-diMe QuinoSiR
HOMO -> LUMO	99.1%	100.2%	97.7%
	Ac-2,6-diMe SiR640	Ac-2,6-diMe JuloSiR	Ac-2,6-diMe QuinoSiR
HOMO -> LUMO	98.4%	98.6%	96.0%

Figure S3. Molecular orbital calculations of **2,6-diMe SiR640**, **2,6-diMe JuloSiR** and **2,6-diMe QuinoSiR** and their acylated derivatives; (a) **2,6-diMe SiR640** and **Ac-2,6-diMe SiR640**, (b) **2,6-diMe JuloSiR** and **Ac-2,6-diMe JuloSiR**, and (c) **2,6-diMe QuinoSiR** and **Ac-2,6-diMe QuinoSiR**. Calculations were performed at the B3LYP/6-31+G* level with water as the solvent. (d) Transition probability between HOMO and LUMO of each compound.

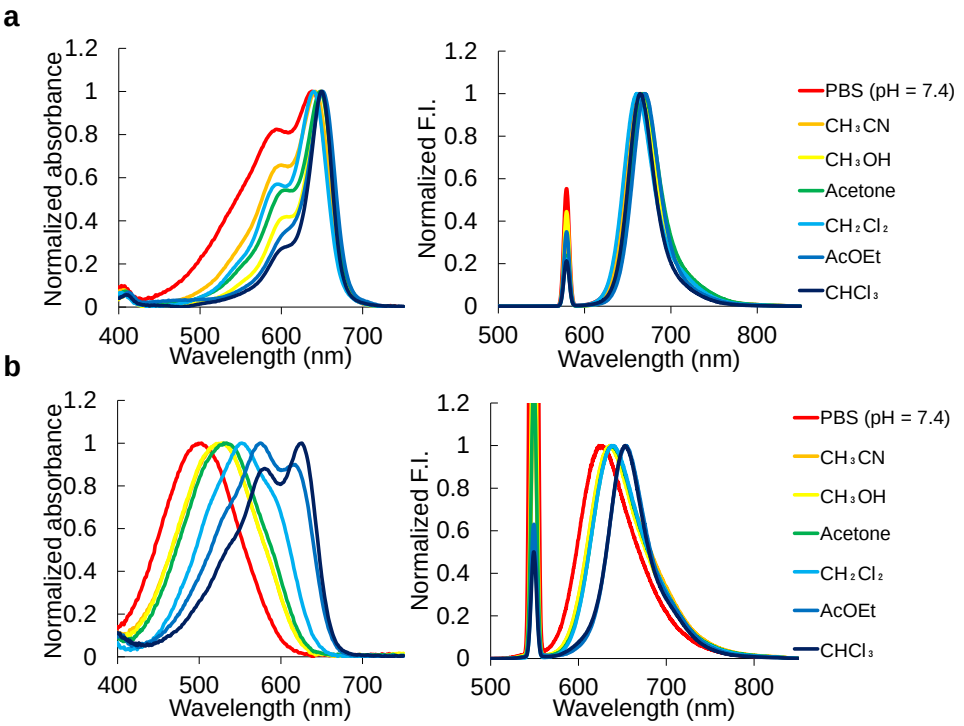

c

	Solvent	PBS	CH_3CN	CH_3OH	Acetone	CH_2Cl_2	AcOEt	$CHCl_3$
	ε (dielectric constant)	80.0	36.6	33.0	20.7	8.9	6.1	4.8
2,6-diMe SiR640	Abs_{max} (nm)	637	642	648	648	640	651	649
	Em_{max} (nm)	662	664	666	668	660	670	665
Ac-2,6-diMe SiR640	Abs_{max} (nm)	503	529	527	533	552	575	626
	Em_{max} (nm)	623	636	636	638	639	654	653

Figure S4. (a,b) Normalized (a) absorption and (b) emission spectra of 1 μM **2,6-diMe SiR640** and **Ac-2,6-diMe SiR640** in organic solvents with various dielectric constants containing 0.1% DMSO as a co-solvent. The excitation wavelengths were 580 nm for **2,6-diMe SiR640** and 550 nm for **Ac-2,6-diMe SiR640**. A sharp fluorescence peaks in (a) and (b) are the Rayleigh scattering of the excitation light. (c) The maximum wavelengths of absorption and emission of **2,6-diMe SiR640** and **Ac-2,6-diMe SiR640** in various organic solvents.

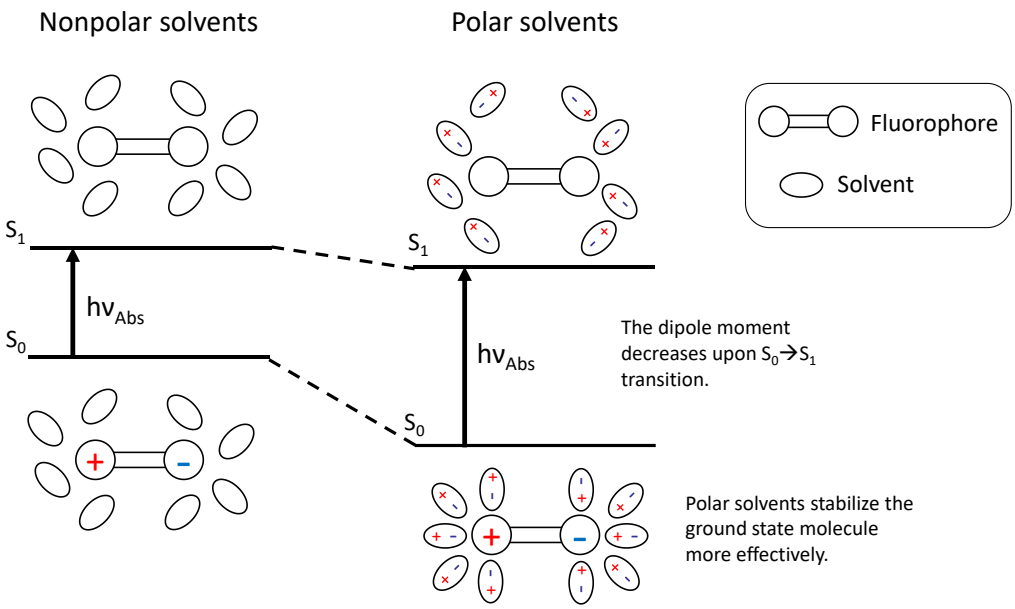

Figure S5. Solvatochromic effects on the absorption wavelength of the environment-sensitive fluorophore.[11-13]

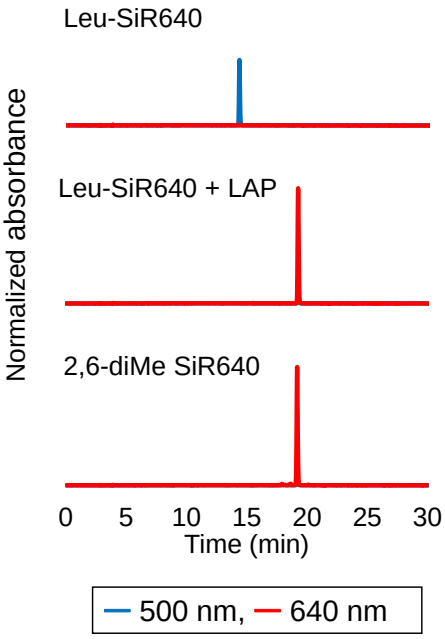

Figure S6. HPLC chromatograms of 10 μM **Leu-SiR640** before and after addition of LAP (5.5 ng), and 10 μM **2,6-diMe SiR640** (eluent: A: H_2O, 0.1% TFA (v/v), B: CH_3CN/H_2O = 80/20, 0.1% TFA (v/v); gradient: A/B = 80/20 to 0/100, 20 min; flow rate: 1.0 mL/min; detection: absorbance at 500 nm and 640 nm).

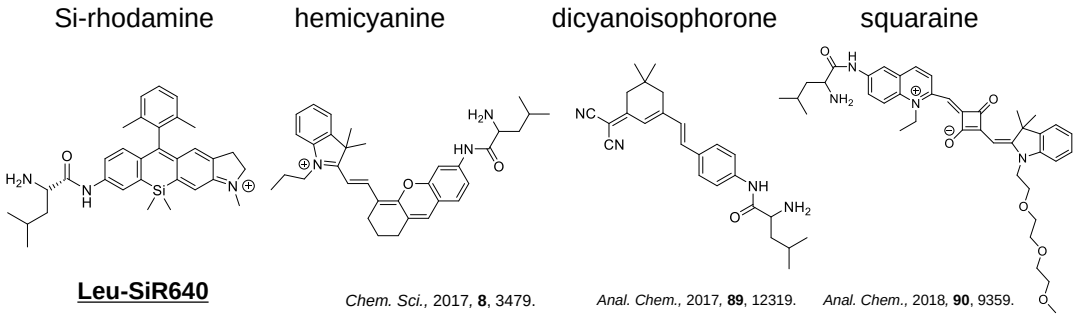

Fluorophore	Si-rhodamine	hemicyanine	discyanophorone	squaraine
$\lambda_{ex/em}$ (nm)	637/660	670/705	460/658	650/710
ΔAbs_{max} (nm)	137	72	65	~ 10
Fold increase	~ 600	32	~ 20	9
K_m (μM)	6.36	123	24.1	10.8

Figure S7. Comparison of NIR fluorescent probes for detecting LAP activity. ΔAbs_{max} indicates the difference between the maximum absorption wavelengths before and after the enzymatic reaction. Fold increase indicates the fold increase of fluorescence after the enzymatic reaction.

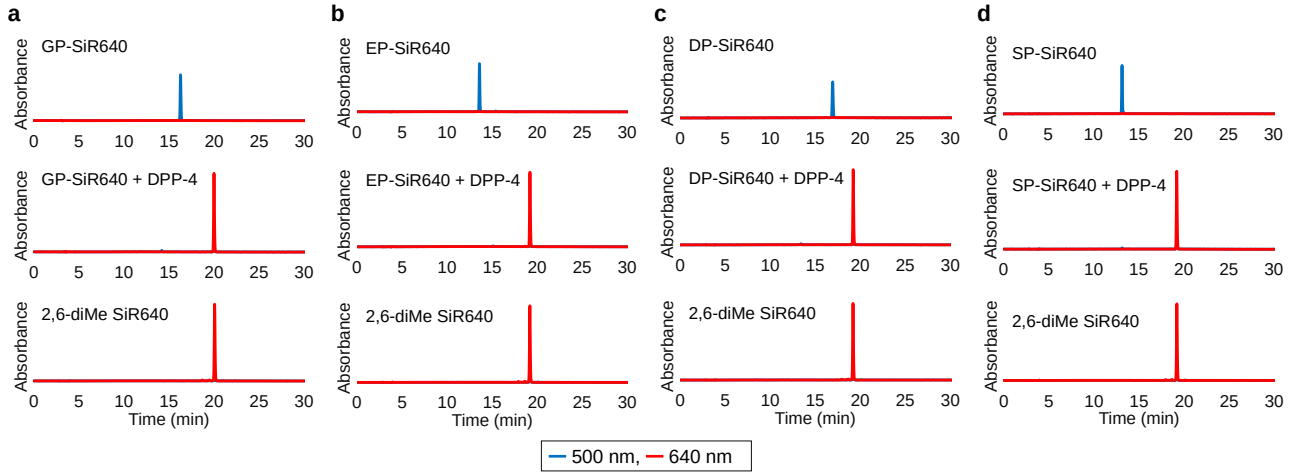

Figure S8. HPLC chromatograms of 10 μM (a) **GP-SiR640**, (b) **EP-SiR640**, (c) **DP-SiR640** and (d) **SP-SiR640** before and after the addition of DPP-4 (0.12 μg), and 10 μM **2,6-diMe SiR640** containing 1% DMSO as a co-solvent (eluent: A: H_2O, 0.1% TFA (v/v), B: CH_3CN/H_2O = 80/20, 0.1% TFA (v/v); gradient: A/B = 80/20 to 0/100, 20 min; flow rate: 1.0 mL/min; detection: absorbance at 500 nm and 640 nm).

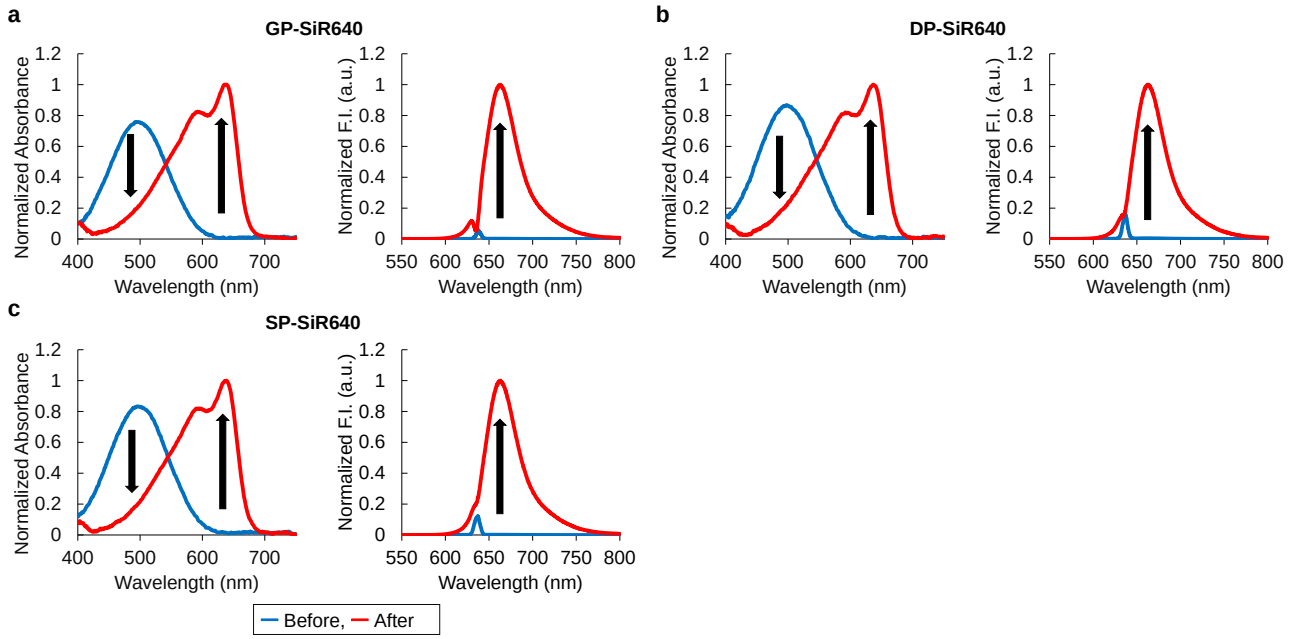

Figure S9. Normalized absorption and emission spectra of 1 μM (a) **GP-SiR640**, (b) **DP-SiR640** and (c) **SP-SiR640** upon addition of DPP-4 (0.24 μg) in 10 mM HEPES buffer (pH = 7.4) containing 0.1% DMSO as a co-solvent. The excitation wavelength was 637 nm. A sharp small fluorescence peaks in (a)-(c) are the Rayleigh scattering of the excitation light.

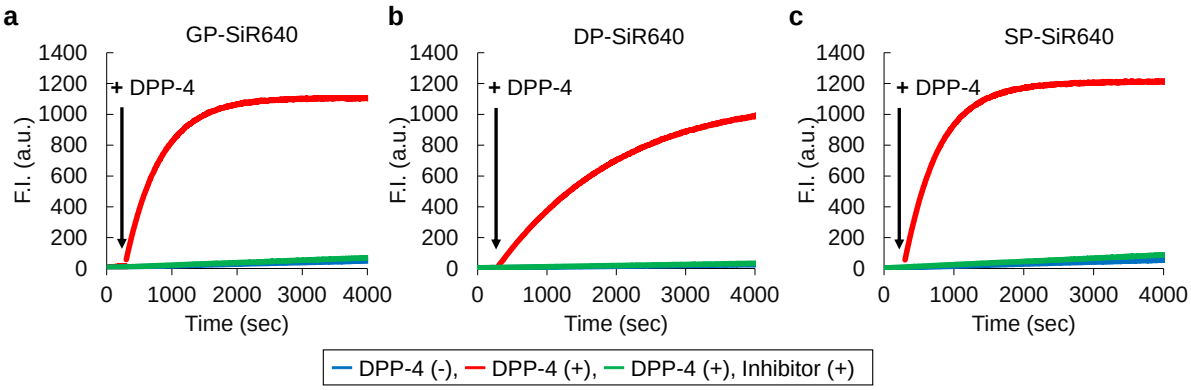

Figure S10. Time-course of the fluorescence intensity of 1 μM (a) **GP-SiR640**, (b) **DP-SiR640** and (c) **SP-SiR640** upon addition of DPP-4 (0.24 μg, at 300 sec) in 10 mM HEPES buffer (pH = 7.4) containing 0.1% DMSO as a co-solvent. The excitation and emission wavelengths were 637 nm and 660 nm, respectively. The concentration of the inhibitor (sitagliptin) was 1.8 μM.

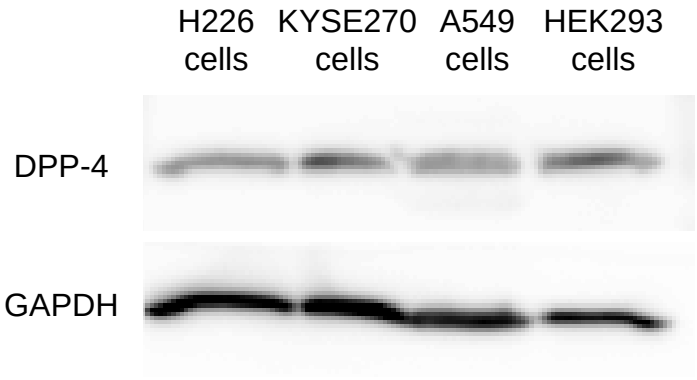

Figure S11. Western blotting analysis for DPP-4 in H226, KYSE270, A549 and HEK293 cells. Rabbit polyclonal DPP4 antibody (Proteintech, 10940-1-AP) and anti-GAPDH mouse monoclonal antibody (Santa Cruz Biotechnology, sc-32233) were used as primary antibodies. The detection was performed by chemiluminescence.

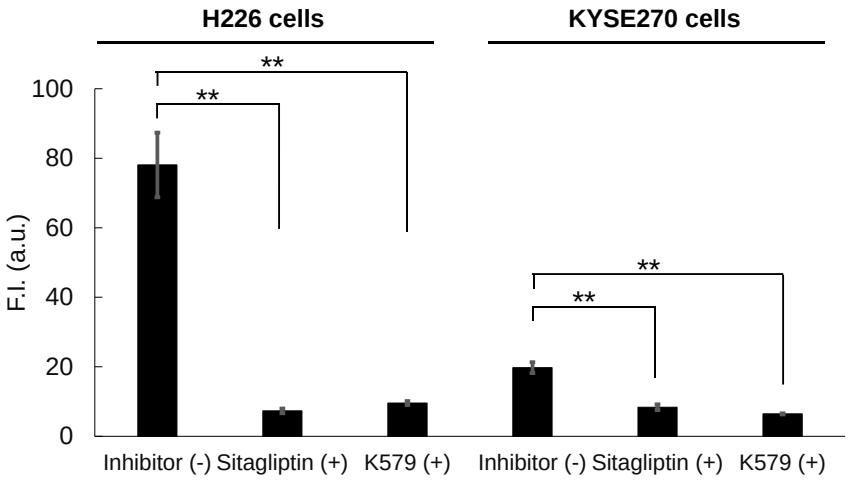

Figure S12. The fluorescence intensities of H226 and KYSE270 cells incubated with 1 μM **EP-SiR640** for 10 min. Error bars represent ±S.E. (n = 4). ** indicates $p < 0.01$ by Student's *t*-test.

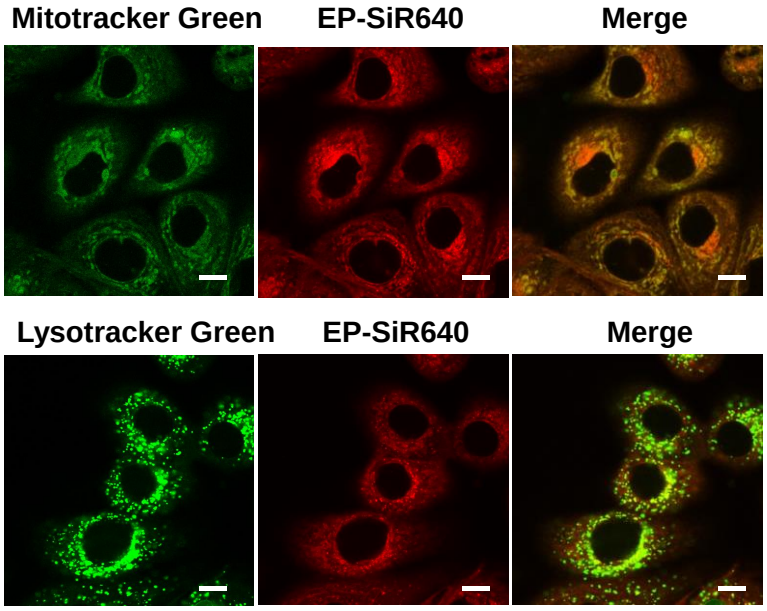

Figure S13. Fluorescence confocal microscopy images of live H226 cells treated with intracellular organelle indicators. Cells were incubated with 1 μM **EP-SiR640** and 100 nM MitoTracker® Green FM containing 0.2% DMSO as a co-solvent for 30 min, or incubated with 1 μM **EP-SiR640** and 50 nM LysoTracker® Green DND26 containing 0.2% DMSO as a co-solvent for 60 min. The excitation and emission wavelengths were 488 and 515-550 nm for MitoTracker® Green FM and LysoTracker® Green DND26, or 633 nm and 660-695 nm for **EP-SiR640**, respectively. Scale bars represent 10 μm.

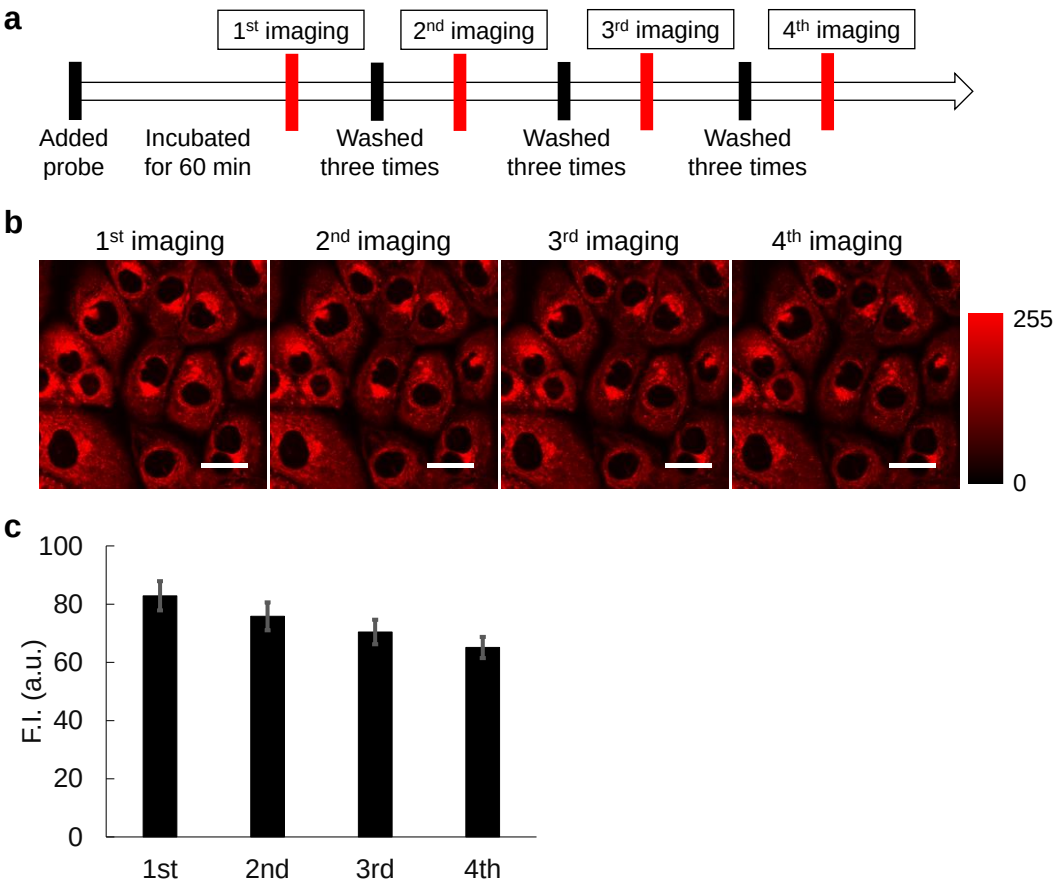

Figure S14. a) Experimental protocol for evaluating the intracellular retention of **EP-SiR640**. H226 cells were incubated with 1 μM **EP-SiR640** containing 0.1% DMSO as a co-solvent for 60 min, then washed with HBSS three times. This washing process was repeated two times. b) Fluorescence confocal microscopy images of live H226 cells. The excitation and emission wavelengths were 633 nm and 660-695 nm, respectively. Scale bars represent 25 μm. c) The fluorescence intensity of H226 cells incubated with **EP-SiR640**. Error bars represent ±S.E. (n = 4).

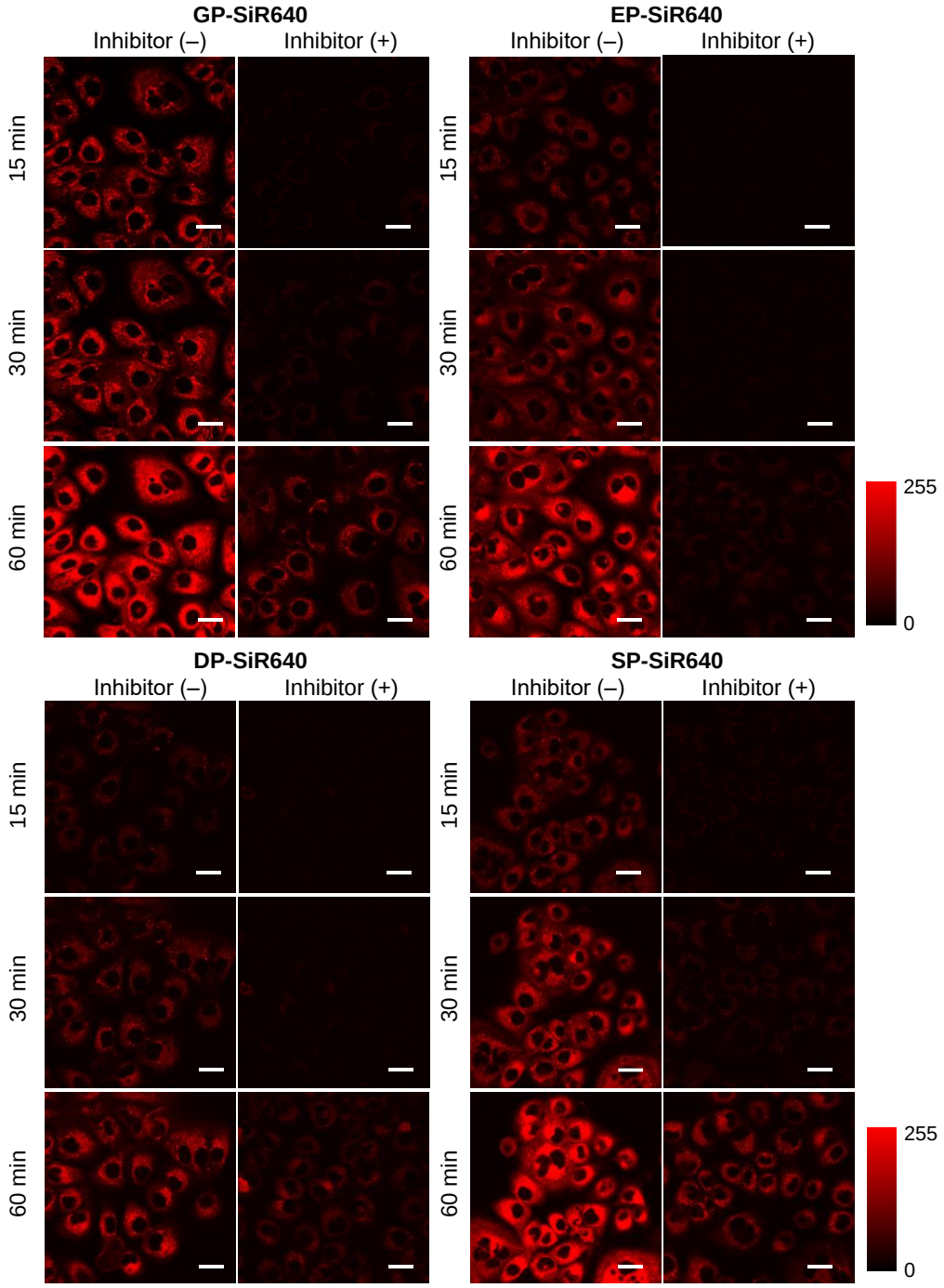

Figure S15. Fluorescence confocal microscopy images of live H226 cells treated with or without DPP-4 inhibitor (sitagliptin). Cells were pre-incubated with 18 μM sitagliptin containing 0.2% DMSO as a co-solvent for 30 min and then incubated with 1 μM **GP-SiR640**, **EP-SiR640**, **DP-SiR640** or **SP-SiR640** containing 0.1% DMSO as a co-solvent for up to 60 min. The excitation and emission wavelengths were 633 nm and 660-695 nm, respectively. Scale bars represent 25 μm.

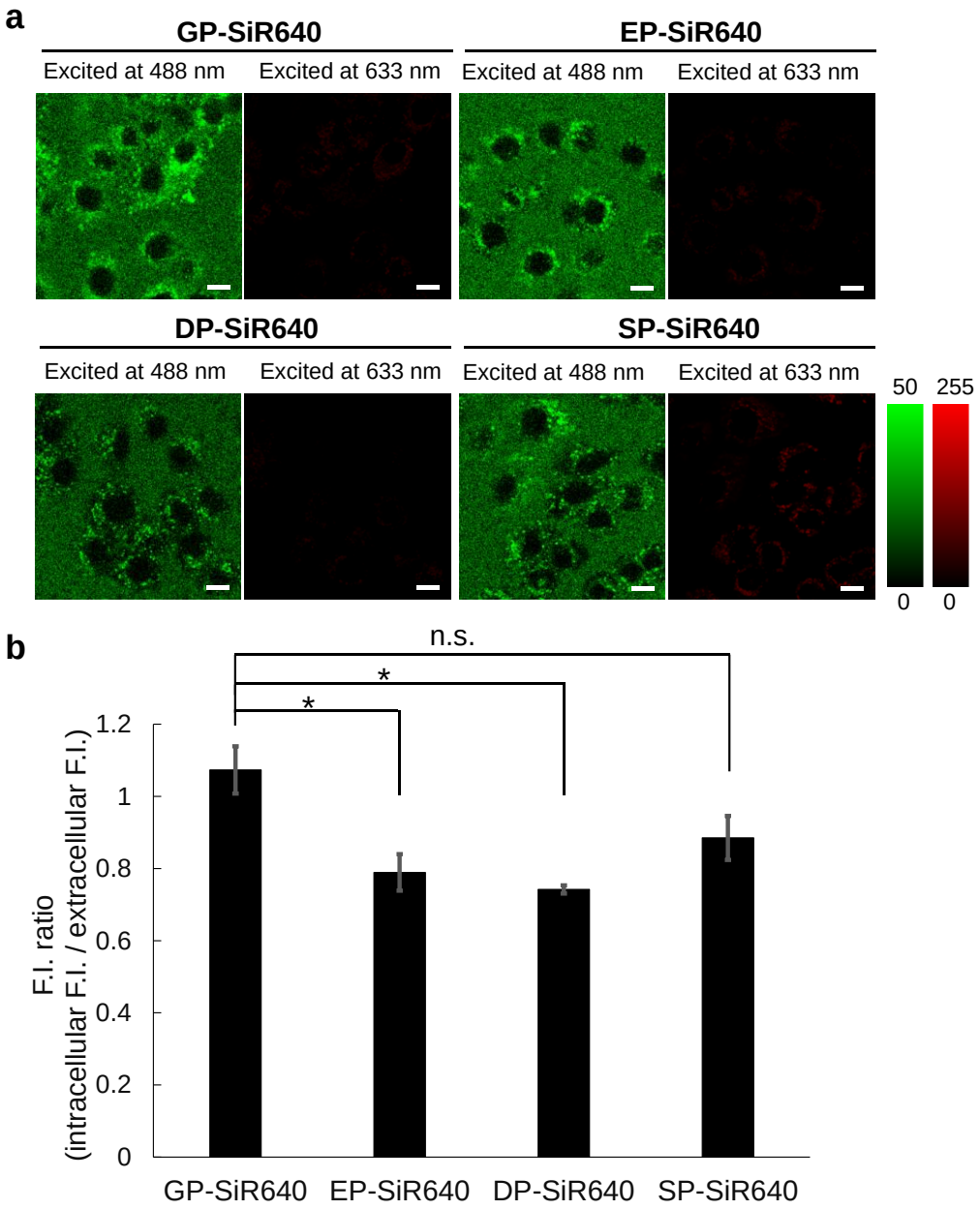

Figure S16. a) Fluorescence confocal microscopy images of live A549 cells. Cells were incubated with 10 μM **GP-SiR640**, **EP-SiR640**, **DP-SiR640** or **SP-SiR640** containing 0.1% DMSO as a co-solvent for 5 min. The excitation and emission wavelengths were 488 nm and 565-600 nm for **GP-SiR640**, **EP-SiR640**, **DP-SiR640** and **SP-SiR640** (before the enzymatic reaction with DPP-4), 633 nm and 660-695 nm for **2,6-diMe SiR640** (after the enzymatic reaction with DPP-4), respectively. Scale bars represent 10 μm. b) The relative fluorescence intensities of A549 cells incubated with each probe for 5 min. Error bars represent ±S.E. (n = 4). * indicates $p < 0.05$ and and n.s. indicates not significant by Student's *t*-test.

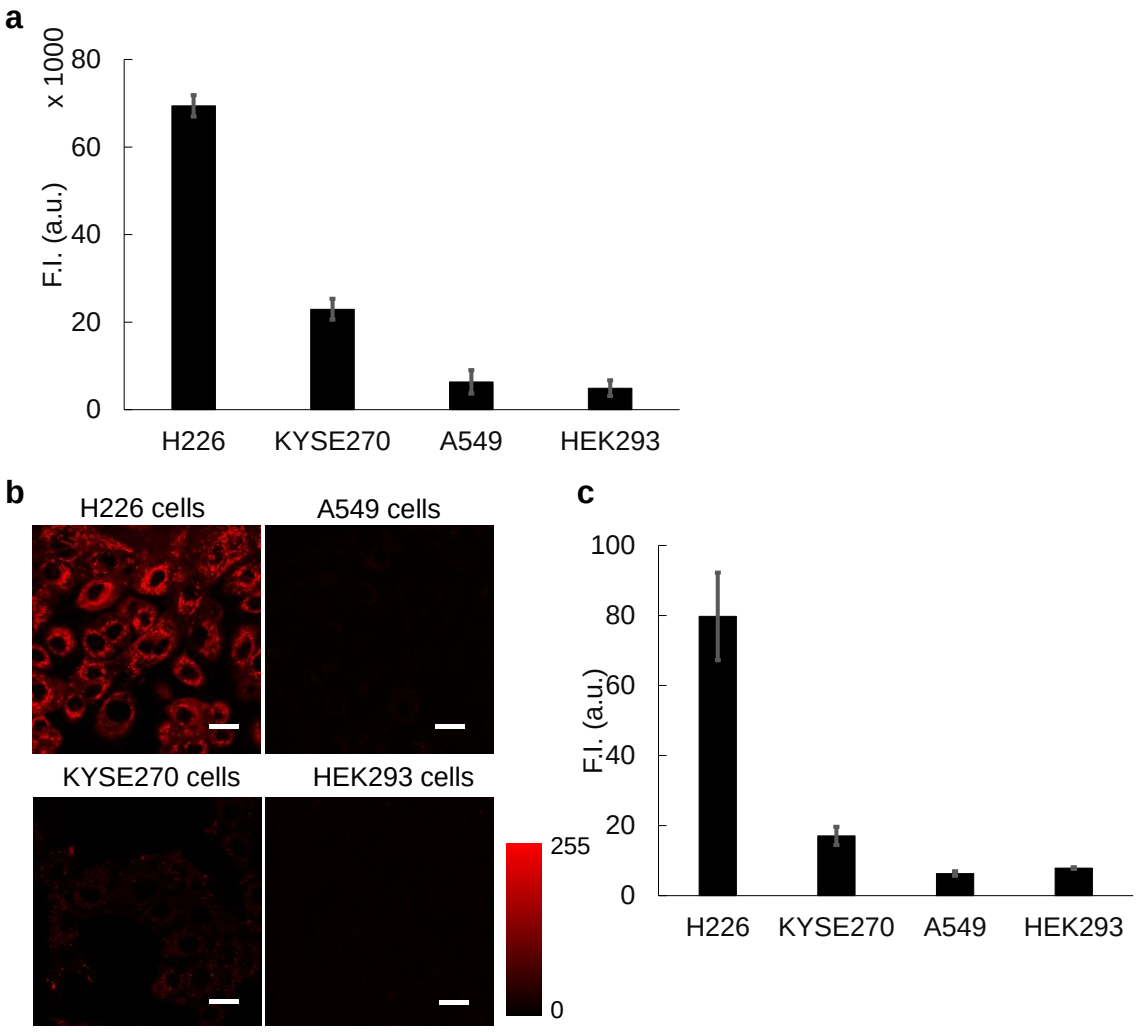

Figure S17. Measurements of the DPP-4 activity in various live cells using **EP-SiR640**. (a) Fluorescence intensity of 1 μM **EP-SiR640** upon addition of 500 ng cell lysate in 10 mM HEPES buffer (pH = 7.4) containing 1% DMSO as a co-solvent. The excitation and emission wavelengths were 620 nm and 685 nm, respectively. Error bars represent ±S.E. (n = 4). (b) Fluorescence confocal microscopy images of live H226, KYSE270, A549 or HEK293 cells. Each cell line was incubated with 1 μM **EP-SiR640** containing 0.1% DMSO as a co-solvent for 10 min. The excitation and emission wavelengths were 633 nm and 660-695 nm, respectively. Scale bars represent 25 μm. (c) The fluorescence intensity of each cell line incubated with **EP-SiR640**. Error bars represent ±S.E. (n = 4).

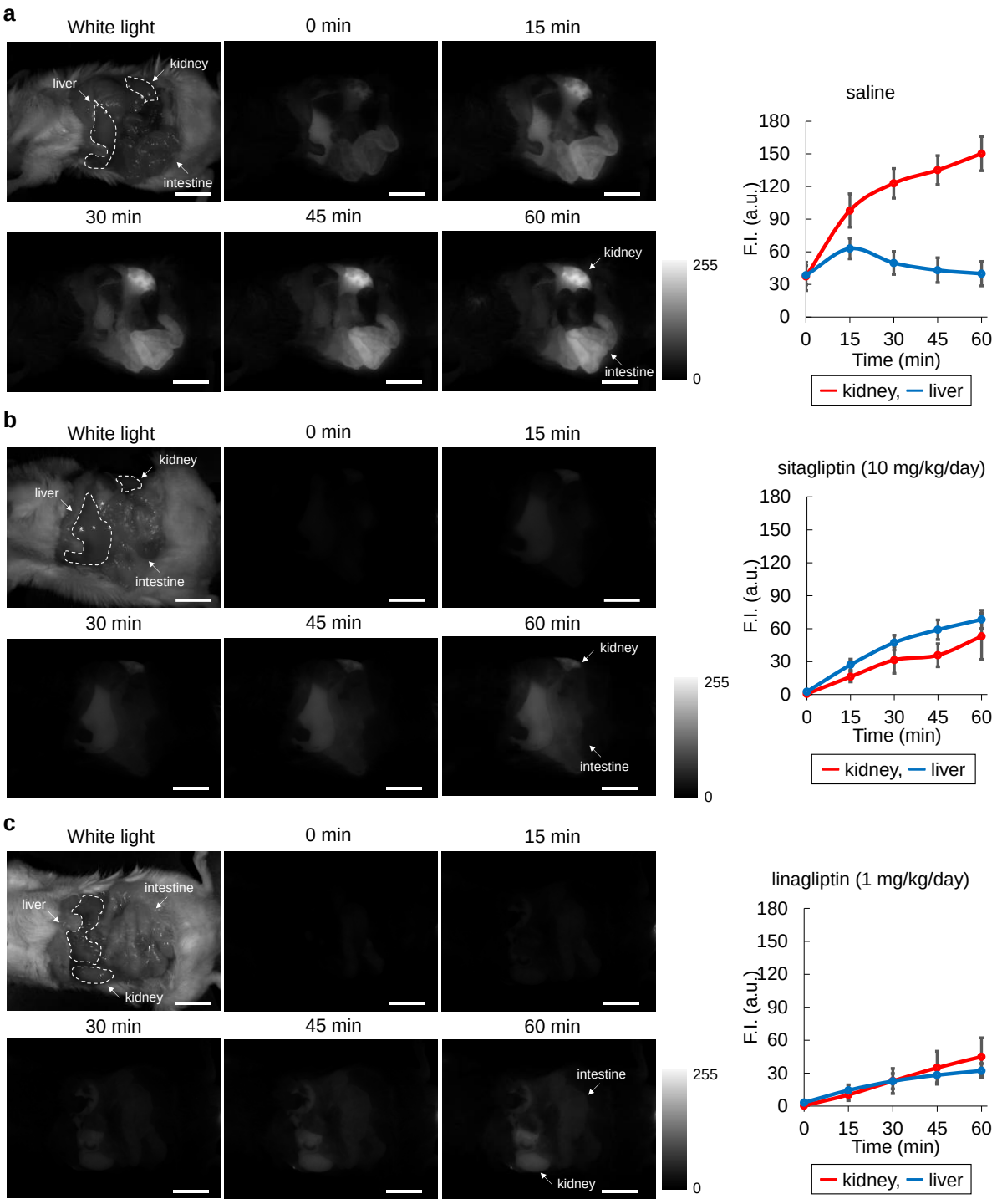

Figure S18. a-c) Fluorescence images of BALB/cAJcl mice (male, 6 weeks old) orally administered with (a) saline, (b) sitagliptin (10 mg/kg/day), or (c) linagliptin (1 mg/kg/day) for 1 week and then intravenously injected with 100 μM **EP-SiR640** in 100 μL saline containing 1% DMSO as a co-solvent via the tail vein. The excitation and emission wavelengths were 635 (616-661) nm and 700 nm, respectively. Scale bars represent 10 mm. The graphs represent the fluorescence intensity changes in kidney and liver. Error bars represent ±S.E. (n = 6).

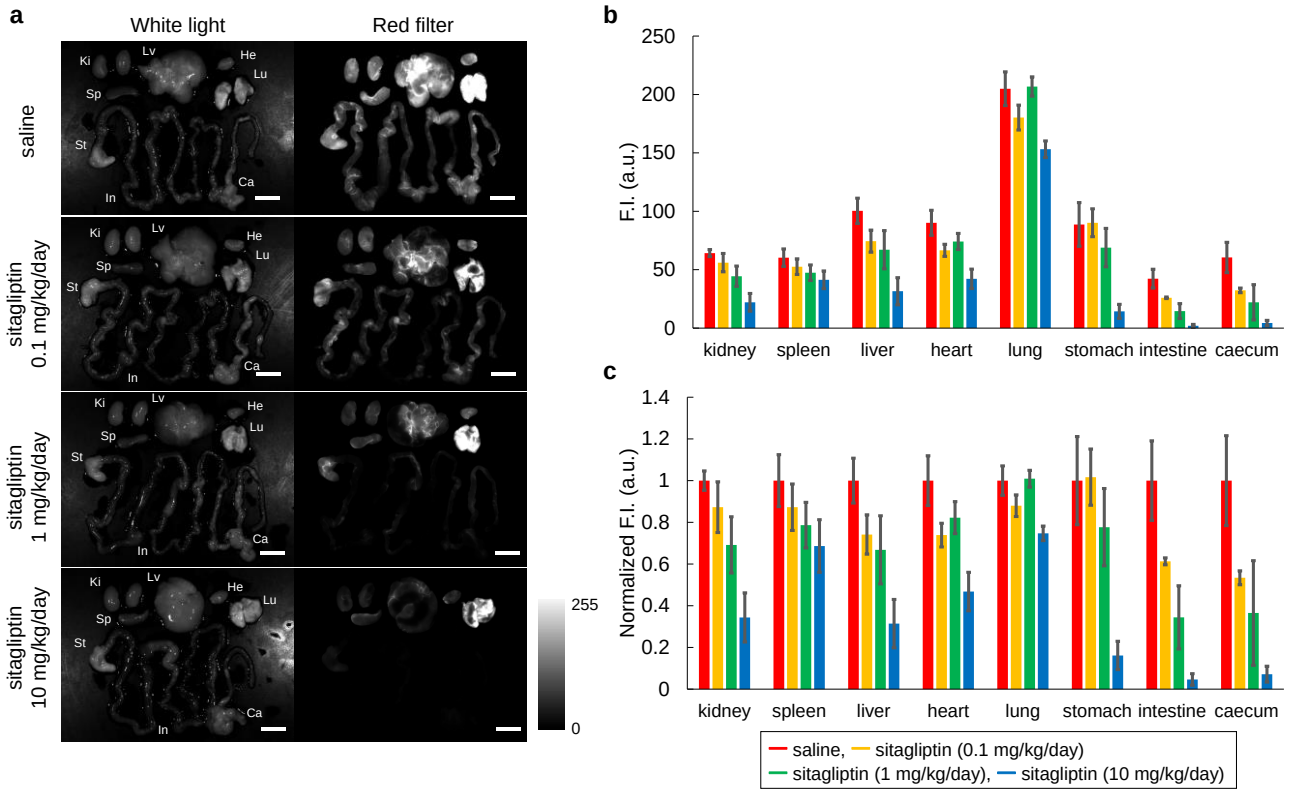

Figure S19. a) Fluorescence images of the organs of BALB/cAJcl mice (male, 6 weeks old) orally administered with saline or various concentrations of sitagliptin (0.1, 1, or 10 mg/kg/day) for 3 days. The removed organs were incubated with 10 μM **EP-SiR640** in 1.5 mL saline containing 1% DMSO as a co-solvent for 20 min. The excitation and emission wavelengths were 635 (616-661) nm and 700 nm, respectively. Scale bars represent 10 mm. Ki: kidney, Sp: spleen, Lv: liver, He: heart, Lu: lung, St: stomach, In: intestine, Ca: caecum. b-c) The fluorescence intensity (b) or the normalized fluorescence intensity (c) of each mouse organ. Error bars represent ±S.E. (n = 4).

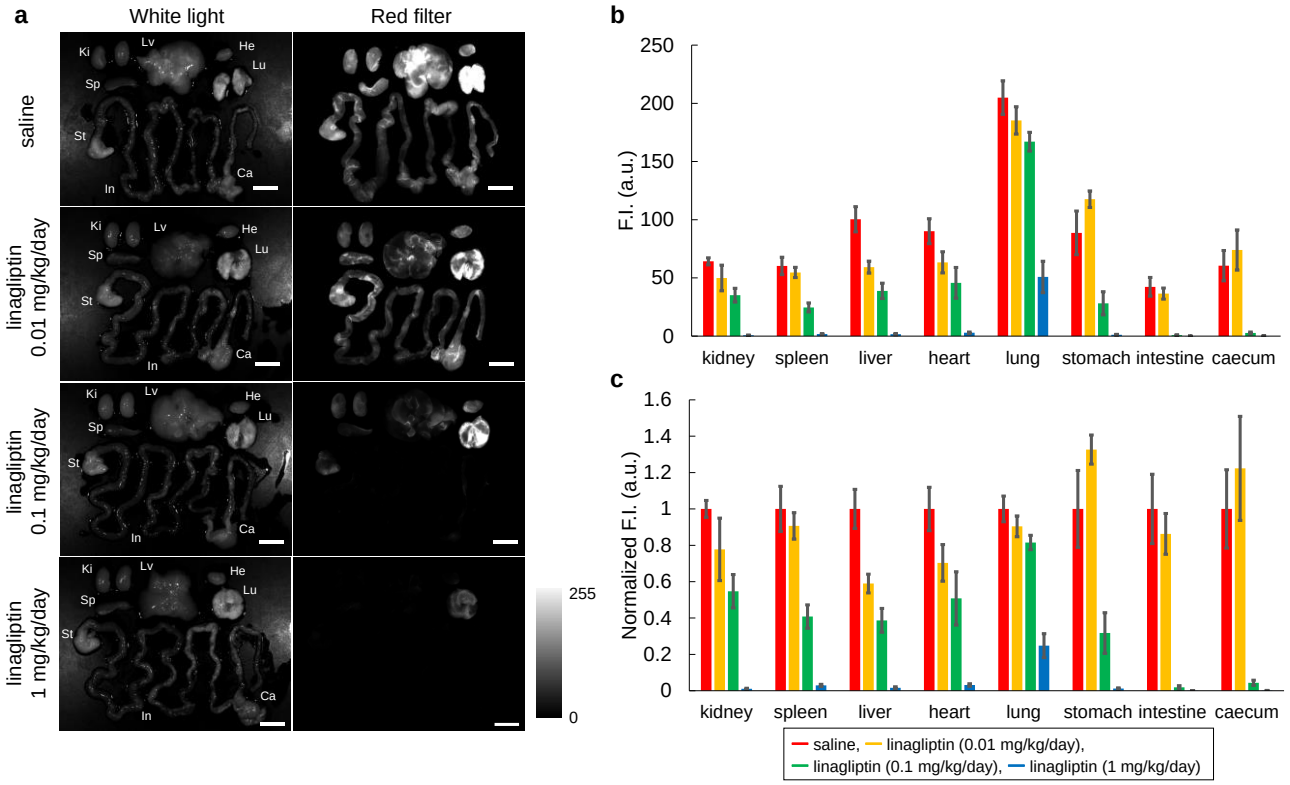

Figure S20. a) Fluorescence images of the organs of BALB/cAJcl mouse (male, 6 weeks old) orally administered with saline or various concentrations of linagliptin (0.01, 0.1, or 1 mg/kg/day) for 3 days. The removed organs were incubated with 10 μM **EP-SiR640** in 1.5 mL saline containing 1% DMSO as a co-solvent for 20 min. The excitation and emission wavelengths were 635 (616-661) nm and 700 nm, respectively. Scale bars represent 10 mm. Ki: kidney, Sp: spleen, Lv: liver, He: heart, Lu: lung, St: stomach, In: intestine, Ca: caecum. b-c) The fluorescence intensity (b) or the normalized fluorescence intensity (c) of each mouse organ. Error bars represent ±S.E. (n = 4).

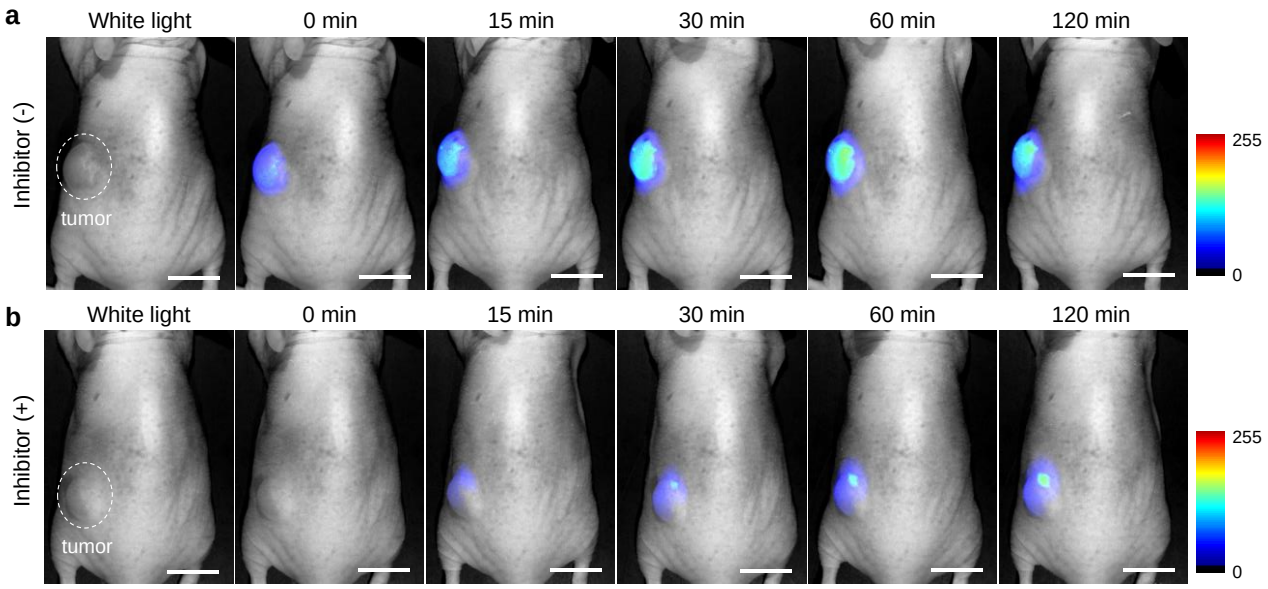

Figure S21. a-b) Fluorescence images of tumor-bearing BALB/cA-nu-nu mice (female, 5 weeks old) intratumorally injected with saline or 0.05 mg sitagliptin in 10 μL saline, then with 100 μM **EP-SiR640** in 10 μL saline containing 1% DMSO as a co-solvent. The excitation and emission wavelengths were 635 (616-661) nm and 700 nm, respectively. Scale bars represent 10 mm.

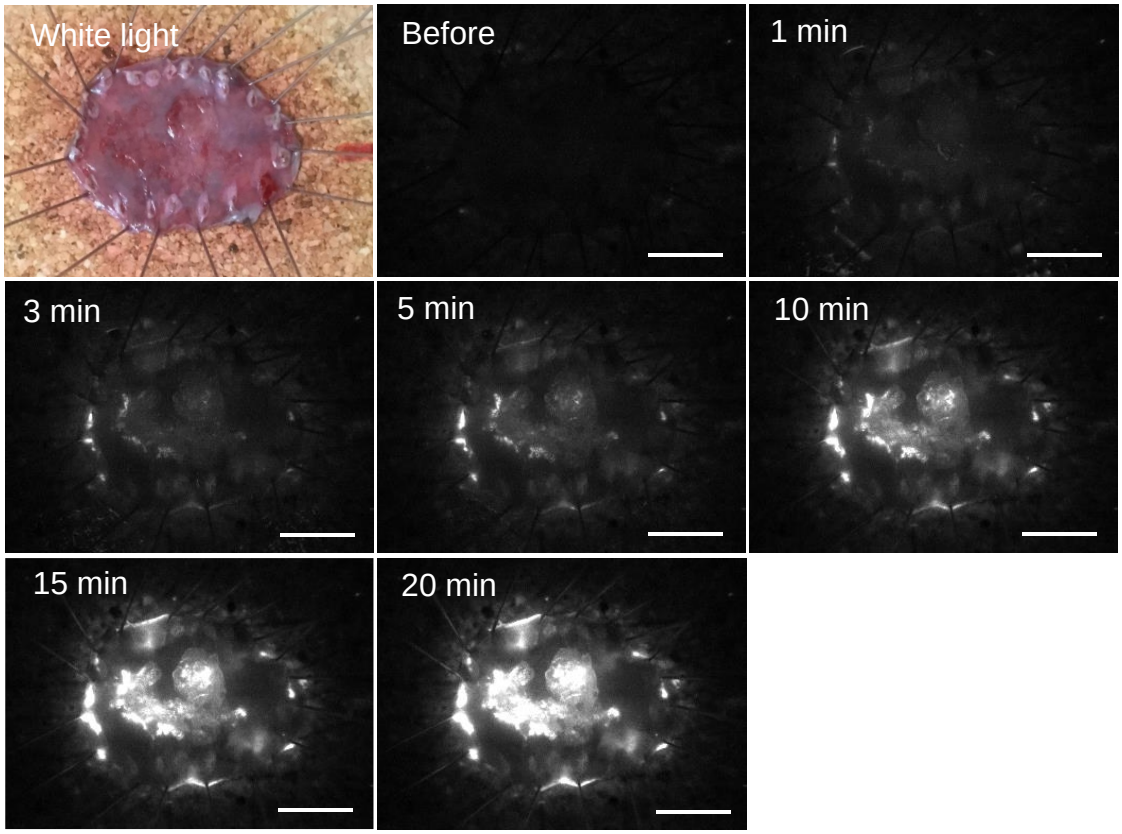

Figure S22. Fluorescence images of esophageal cancer in a clinical specimen resected by ESD. 50 μM **EP-SiR640** in PBS (pH = 7.4) containing 0.5% DMSO as a co-solvent was added to the specimen. The excitation and emission wavelengths were 635 (616-661) nm and 700 nm, respectively. Scale bars represent 10 mm.

No.1: The ESD specimen of esophageal cancer was stained with Lugol's staining solution, then sprayed with **EP-SiR640** after the washing process.

The boundary between the tumor and normal tissues in this fluorescence image is clear, and is in good agreement with that in the Lugol's staining, as well as with the pathological diagnosis and distribution of the tumor.

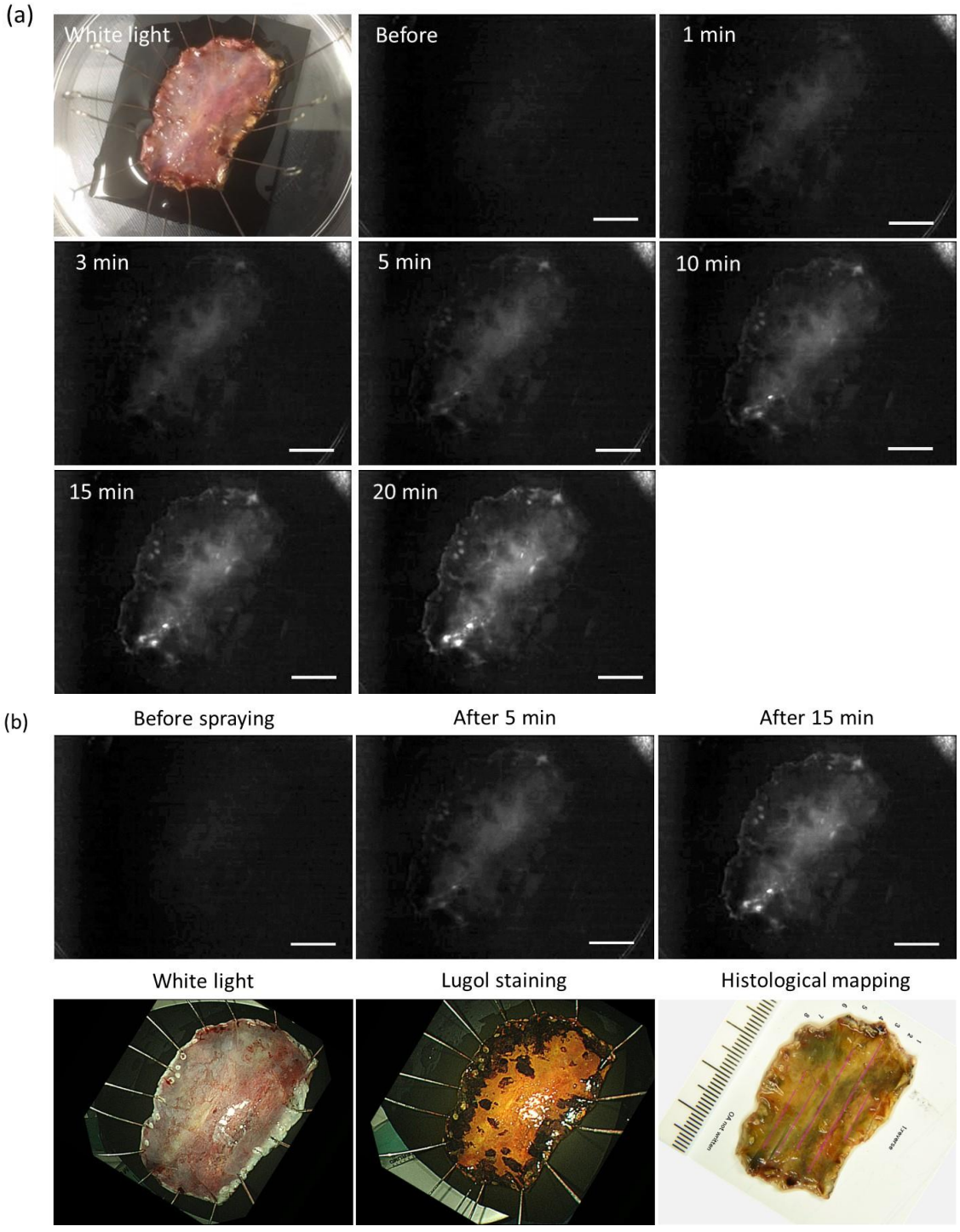

No.2: The ESD specimen of esophageal cancer was sprayed with **EP-SiR640**, then stained with Lugol's staining solution after the washing process.

The boundary between the tumor and normal tissues in this fluorescence image is clear, and is in good agreement with that in the Lugol's staining, as well as with the pathological diagnosis and distribution of the tumor. This specimen showed a large fluorescence increase compared with other specimens. The invasion depth of the tumor was SM2, which was the deepest among the specimens, and this might account for the intense fluorescence.

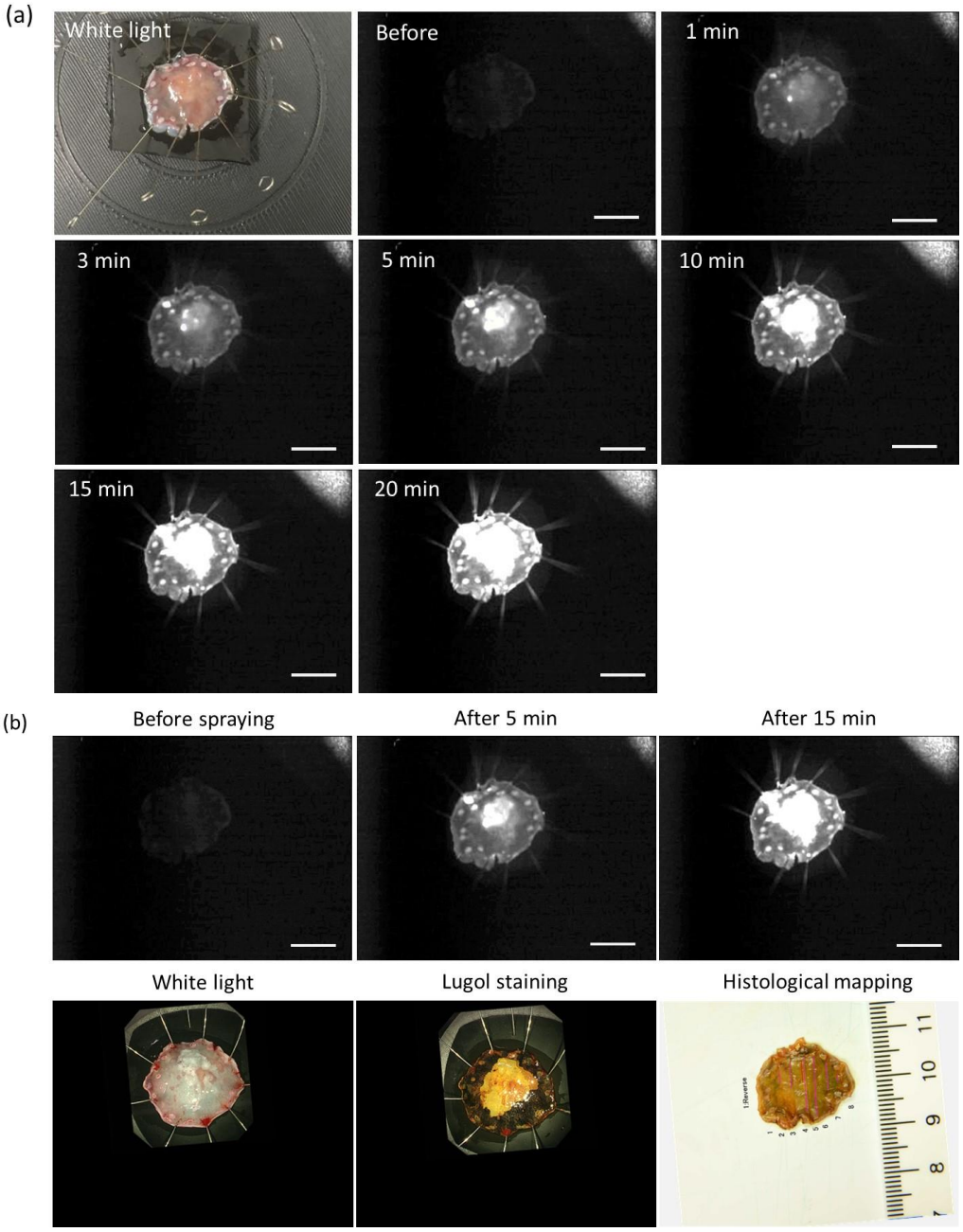

No.3: The ESD specimen of esophageal cancer was sprayed with **EP-SiR640**, then stained with Lugol's staining solution after the washing process.

The boundary between the tumor and normal tissues in this fluorescence image is basically in good ag reement with that in the Lugol's staining, as well as with the pathological diagnosis and distribution of th e tumor., though some parts of the boundary between the tumor and normal tissues in this fluorescence i mage are unclear.

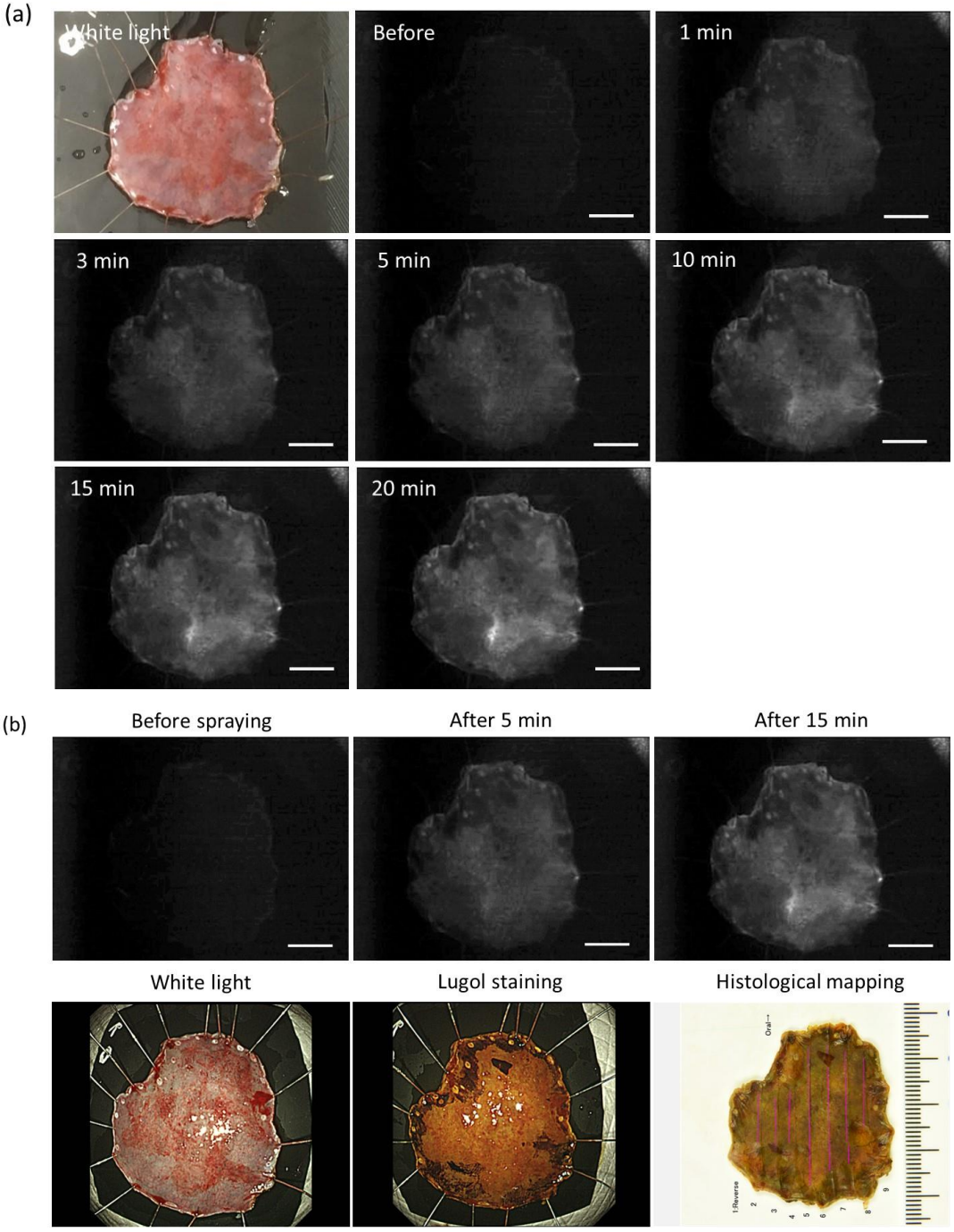

No.4: The ESD specimen of esophageal cancer was stained with Lugol's staining solution, then sprayed with **EP-SiR640** after the washing process.

Although a part of tumor (the center part of the fluorescence image) was not detected in the fluoresce nce image, most of the tumor was imaged. The tumor region showing saturated fluorescence signals may have been attached by the traction ESD method using clips or may include intraductal involvement.

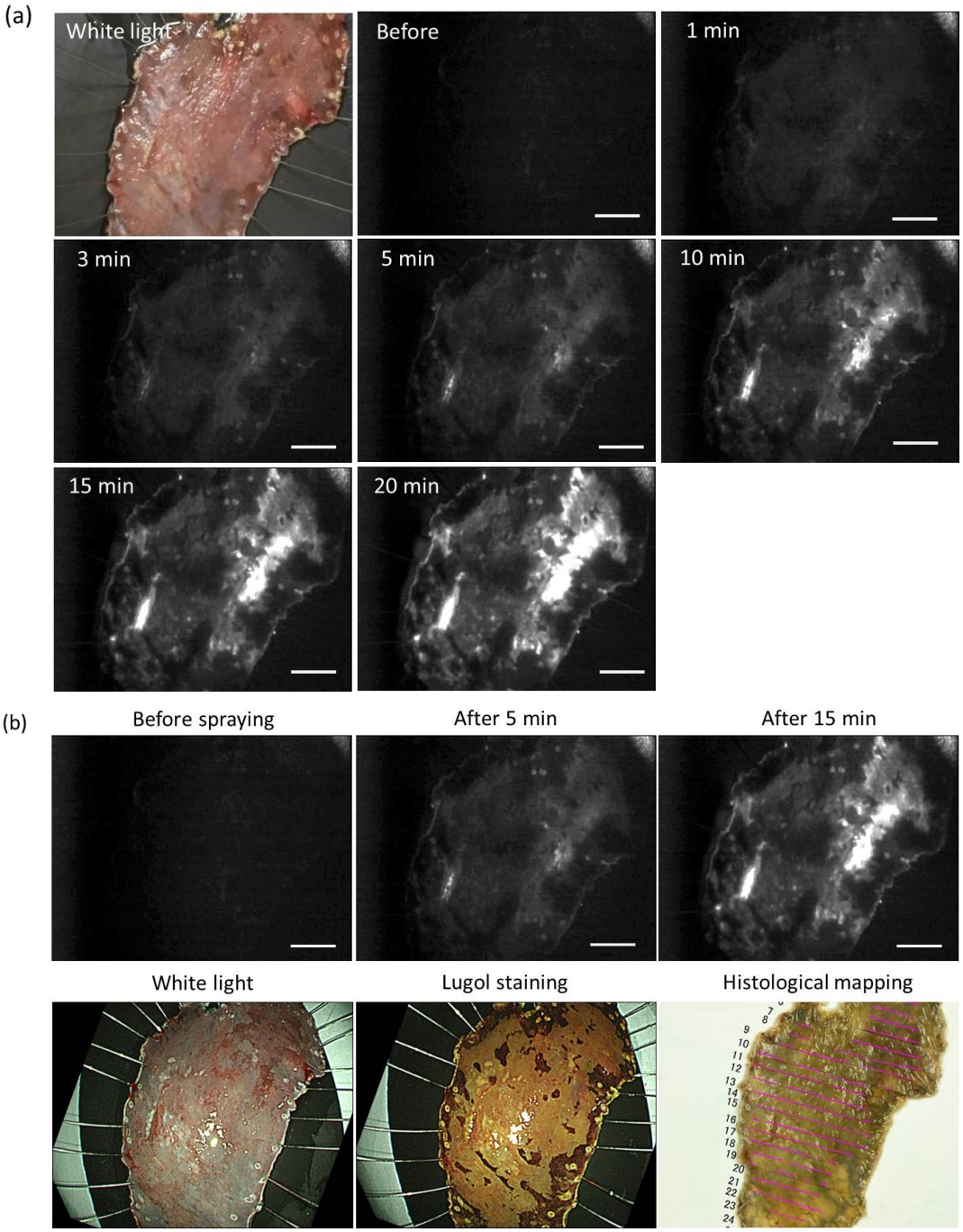

No.5: The ESD specimen of esophageal cancer was sprayed with **EP-SiR640**, then stained with Lugol's staining solution after the washing process.

It was difficult to identify the boundary between the tumor and normal tissues in this fluorescence im age. Although a large fluorescence increase was observed in some parts of the tumor, a fluorescence incre ase was observed all over the specimen.

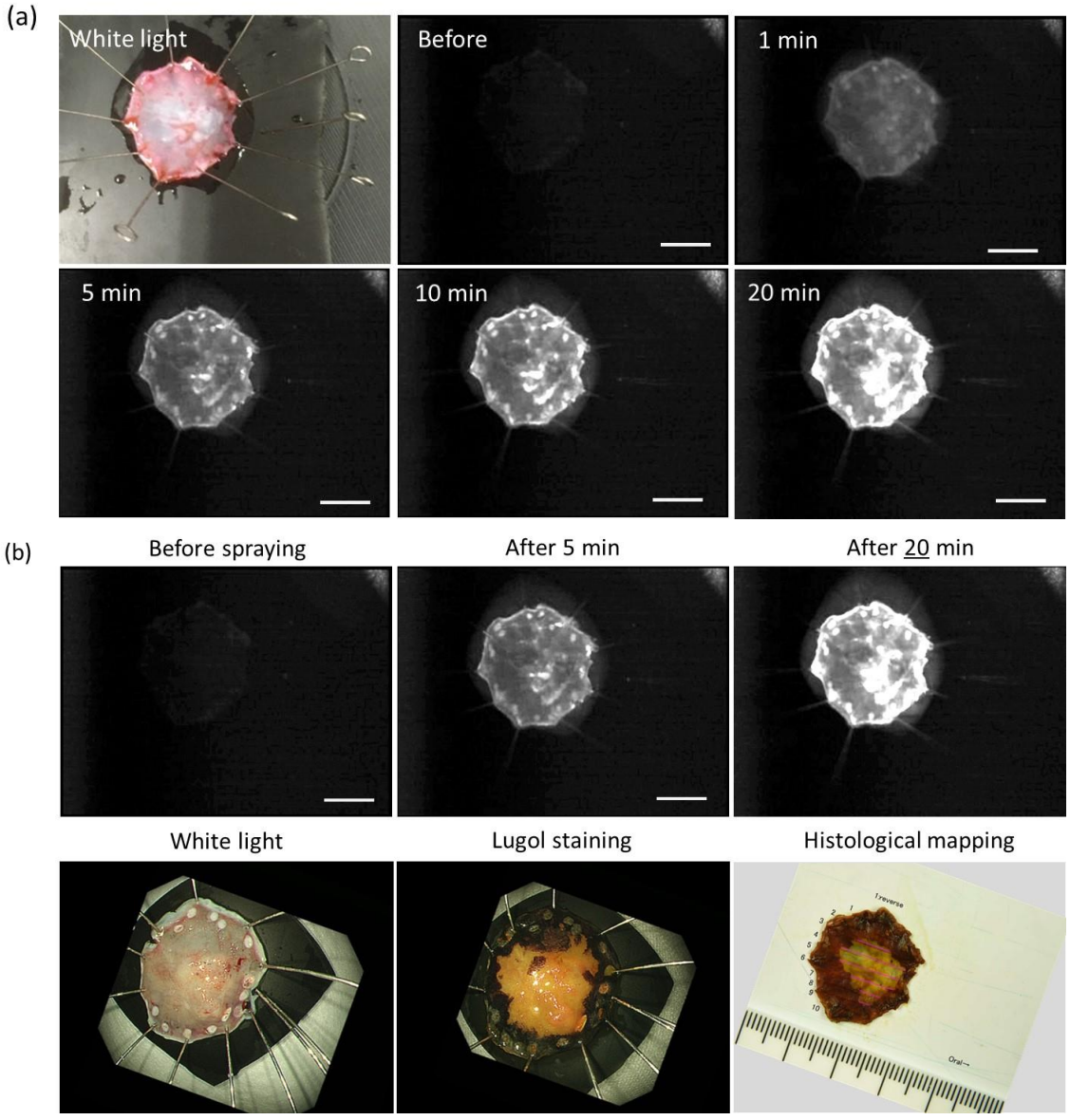

No.6: The ESD specimen of esophageal cancer was stained with Lugol's staining solution, then sprayed with **EP-SiR640** after the washing process.

It was difficult to identify the boundary between the tumor and normal tissues in this fluorescence im age. Although a fluorescence increase was observed in the tumor, the normal region at the lower part of the specimen also showed a fluorescence increase.

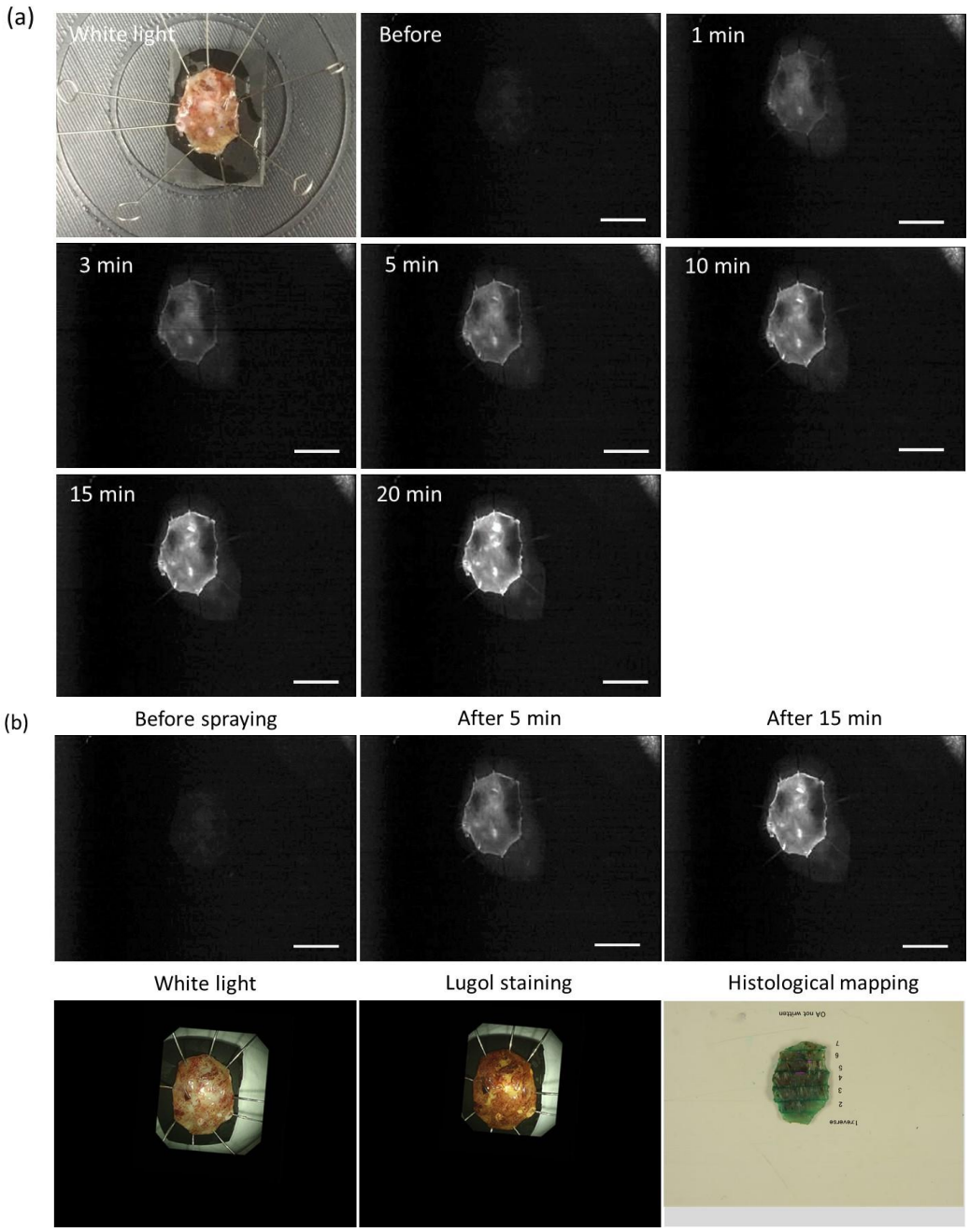

Figure S23. Fluorescence images of esophageal cancer in clinical specimens resected by ESD. Each specimen was sprayed with 50 μM EP-SiR640 in PBS (pH = 7.4) containing 0.5% DMSO as a co-solvent, then the fluorescence

imaging was performed for 20 min using a Discovery™ imaging system. The excitation and emission wavelengths were 630 nm and 670 nm, respectively. Scale bars represent 10 mm. (b) Fluorescence images after 5 min and 15 (or 20) min after spraying of EP-SiR640, white-light images before and after Lugol dye staining and histological mapping of esophageal cancer in ESD specimens. Pink line indicates the tumor distribution.

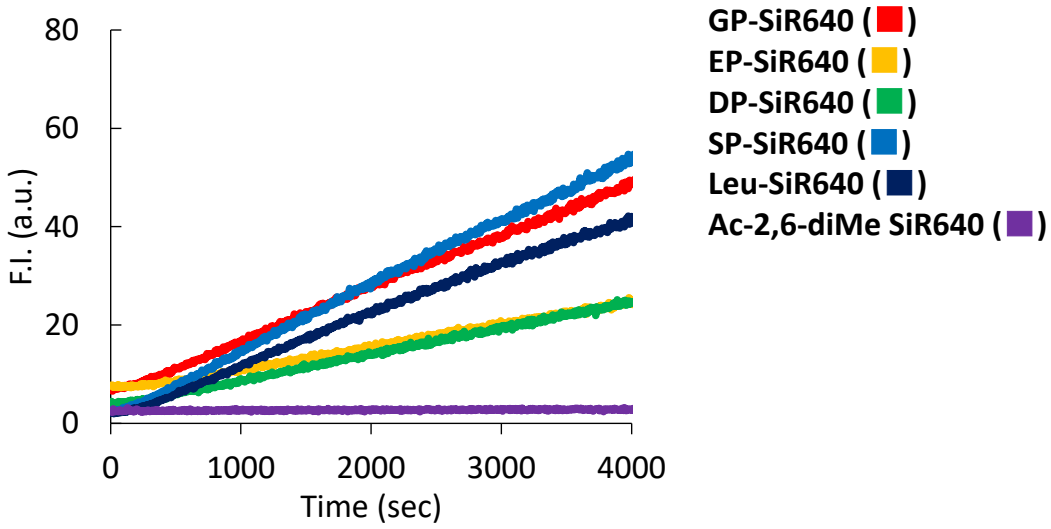

Figure S24. Stability experiment of the acylated SiR640s. Each probe (1 μM) was dissolved in 10 mM HEPES buffer (pH = 7.4) containing 0.1% DMSO as a co-solvent. Time-course of the fluorescence intensity of each probe solution is shown. The vertical axis is largely magnified, compared to Figure 2c, Figure 3c and Figure S10. The excitation and emission wavelengths were 637 nm and 660 nm, respectively.

Note: The non-enzymatic fluorescence increases of **GP-SiR640**, **SP-SiR640** and **Leu-SiR640** were somewhat larger than those of **EP-SiR640** and **DP-SiR640**, on the other hand, **Ac-2,6-diMe SiR640** showed almost no non-enzymatic fluorescence increase. Thus, the non-enzymatic fluorescence increase of the acylated SiR640s was depended on the cleaved group, and the stability of the probe may be controlled by the structure of the cleaved group.

Table S1. Pathological diagnosis of each esophageal cancer patient

No.	Location	Macroscopic type	Size (mm)	Deapth of invasion	Lymphatic (ly) or venous (v) invasion	Pathological horizontal margin (pHM) or vertical margin (pVM)
1	Mt	0-IIc	36 × 20	LPM	ly0, v0	pHM0, pVM0
2	Ut	0-IIc	13 × 12	SM2	ly1, v1	pHM0, pVMX
3	MtLt	0-IIc	30 × 26	MM	ly0, v0	pHM0, pVM0
4	MtLt	0-IIc	69 × 31	LPM	ly0, v0	pHM0, pVM0
5	Mt	0-IIa+IIc	13 × 13	MM	ly0, v0	pHM0, pVM0
6	Lt	0-IIc	5 × 3	EP	ly0, v0	pHM0, pVM0

Cartesian Coordinates and Total Electron Energies

2,6-diMe SiR640 (8)

LUMO -3.28 eV

HOMO -5.74 eV

E(RB3LYP) = -1407.17794764 a.u.

Center Number	Atomic Number	Atomic Type	Coordinates (Angstroms) X	Y	Z
1	6	0	3.422650	-0.540282	-0.029028
2	6	0	2.436737	-1.559874	-0.027864
3	6	0	1.092244	-1.228044	-0.025976
4	6	0	0.674270	0.156765	-0.020804
5	6	0	1.708832	1.165917	-0.026711
6	6	0	3.030103	0.830778	-0.031511
7	6	0	-0.689066	0.570535	-0.007151
8	6	0	-1.857285	-0.275262	0.004019
9	6	0	-1.812880	-1.712618	-0.000054
10	6	0	-2.990192	-2.440920	0.015443
11	1	0	-2.960019	-3.529119	0.011490
12	6	0	-4.268620	-1.819566	0.036349
13	6	0	-4.317790	-0.403196	0.038348
14	6	0	-3.152344	0.329323	0.022395
15	1	0	2.744737	-2.601520	-0.020801
16	1	0	1.429380	2.213480	-0.026405

17	1	0	-5.279973	0.101790	0.053121
18	1	0	-3.234097	1.409891	0.025006
19	14	0	-0.170222	-2.627401	-0.027744
20	7	0	4.760789	-0.656209	-0.029680
21	6	0	-0.001405	-3.659013	-1.599768
22	1	0	-0.115269	-3.038223	-2.495837
23	1	0	0.982453	-4.142375	-1.641495
24	1	0	-0.763637	-4.447183	-1.630799
25	6	0	0.030463	-3.699526	1.512954
26	1	0	-0.064728	-3.102285	2.427007
27	1	0	-0.731386	-4.488228	1.539166
28	1	0	1.014300	-4.184588	1.522440
29	6	0	4.277935	1.689281	-0.063942
30	1	0	4.290667	2.441240	0.730458
31	1	0	4.362151	2.220261	-1.019034
32	6	0	5.423133	0.658032	0.101601
33	1	0	5.901936	0.719223	1.087389
34	1	0	6.202313	0.752073	-0.660915
35	6	0	5.530476	-1.882042	0.075595
36	1	0	4.948111	-2.729015	-0.289933
37	1	0	6.434795	-1.791636	-0.533177
38	1	0	5.824734	-2.070149	1.116787
39	7	0	-5.400177	-2.560942	0.052517
40	1	0	-6.313680	-2.128743	0.072267
41	6	0	-0.945126	2.057943	-0.002144
42	6	0	-1.076695	2.746536	-1.228678

43	6	0	-1.051638	2.743061	1.228771
44	6	0	-1.316334	4.127689	-1.202459
45	6	0	-1.291774	4.124256	1.211317
46	6	0	-1.423822	4.815769	0.006625
47	1	0	-1.419026	4.664199	-2.142818
48	1	0	-1.375352	4.658082	2.155085
49	1	0	-1.610087	5.886732	0.010047
50	6	0	-0.909600	2.020177	2.550571
51	1	0	-1.652536	1.220611	2.658072
52	1	0	0.078045	1.554013	2.652795
53	1	0	-1.040415	2.714298	3.386106
54	6	0	-0.961305	2.027393	-2.555103
55	1	0	-1.706089	1.227917	-2.649721
56	1	0	-1.109156	2.723792	-3.385883
57	1	0	0.024155	1.561751	-2.678596
58	1	0	-5.369310	-3.571285	0.059970

Ac-2,6-diMe SiR640 (9)

LUMO -3.51 eV

HOMO -6.13 eV

E(RB3LYP) = -1559.84338708 a.u.

Center Number	Atomic Number	Atomic Type	Coordinates (Angstroms) X	Y	Z

1	6	0	3.602002	-1.725266	0.009968
2	6	0	2.284054	-2.263689	0.006552
3	6	0	1.191080	-1.423306	0.004227
4	6	0	1.368850	0.021095	0.003120
5	6	0	2.728520	0.529080	0.004778
6	6	0	3.798968	-0.307275	0.008396
7	6	0	0.301341	0.941264	0.000651
8	6	0	-1.128932	0.631178	0.000024
9	6	0	-1.660486	-0.692710	-0.000311
10	6	0	-3.041633	-0.897453	-0.000749
11	1	0	-3.446390	-1.900950	-0.001012
12	6	0	-3.944490	0.183947	-0.000624
13	6	0	-3.426063	1.492636	-0.000511
14	6	0	-2.060220	1.704869	-0.000258
15	1	0	2.149812	-3.341000	0.001903
16	1	0	2.892028	1.600648	0.003519
17	1	0	-4.101643	2.344541	-0.000540
18	1	0	-1.704986	2.728205	-0.000145
19	14	0	-0.532614	-2.194275	-0.000293
20	7	0	4.771389	-2.368133	0.014001
21	6	0	-0.785178	-3.226858	-1.559342
22	1	0	-0.630259	-2.626727	-2.463155
23	1	0	-0.086099	-4.071668	-1.584639
24	1	0	-1.803468	-3.633605	-1.589046
25	6	0	-0.790975	-3.230558	1.555341
26	1	0	-0.638805	-2.632641	2.461093

27	1	0	-1.809591	-3.636778	1.580684
28	1	0	-0.092487	-4.075833	1.581084
29	6	0	5.286332	-0.025124	0.018807
30	1	0	5.583477	0.517292	0.922271
31	1	0	5.592408	0.578663	-0.840958
32	6	0	5.921037	-1.438108	-0.023841
33	1	0	6.573019	-1.643230	0.831405
34	1	0	6.493859	-1.620706	-0.939924
35	6	0	4.997828	-3.802868	-0.008642
36	1	0	4.064245	-4.340954	0.152864
37	1	0	5.423595	-4.100776	-0.974127
38	1	0	5.703605	-4.070182	0.784282
39	7	0	-5.336130	0.043875	-0.000513
40	1	0	-5.849506	0.917364	-0.000742
41	6	0	-6.107651	-1.100644	0.000235
42	8	0	-5.629195	-2.234861	0.000745
43	6	0	-7.604166	-0.865076	-0.000029
44	1	0	-8.034996	-1.350943	0.881518
45	1	0	-7.886950	0.190616	0.003444
46	1	0	-8.033675	-1.344591	-0.885747
47	6	0	0.653771	2.407553	-0.000983
48	6	0	0.812746	3.083811	-1.231167
49	6	0	0.811670	3.087180	1.227484
50	6	0	1.130669	4.449041	-1.210700
51	6	0	1.129551	4.452362	1.203546
52	6	0	1.288372	5.132334	-0.004445

53	1	0	1.253748	4.977056	-2.153340
54	1	0	1.251707	4.983002	2.144832
55	1	0	1.533562	6.191318	-0.005786
56	6	0	0.651761	2.373393	2.552123
57	1	0	-0.331298	1.895657	2.641435
58	1	0	1.403312	1.584431	2.679654
59	1	0	0.760326	3.075395	3.384160
60	6	0	0.653836	2.366405	-2.553972
61	1	0	-0.329867	1.889997	-2.643432
62	1	0	0.764800	3.065803	-3.387886
63	1	0	1.404304	1.575866	-2.678002

2,6-diMe JuloSiR (12)

LUMO -3.24 eV

HOMO -5.71 eV

E(RB3LYP) = -1523.92334152 a.u.

Center Number	Atomic Number	Atomic Type	Coordinates (Angstroms) X	Y	Z
1	6	0	3.101183	0.029466	-0.002810
2	6	0	2.236799	-1.132083	-0.028410
3	6	0	0.854986	-1.001868	0.000590
4	6	0	0.249016	0.315757	0.031192
5	6	0	1.140266	1.436504	0.057333

6	6	0	2.505406	1.332799	0.054518
7	6	0	-1.151118	0.582832	0.022846
8	6	0	-2.220052	-0.379594	-0.028165
9	6	0	-2.005278	-1.796888	-0.063653
10	6	0	-3.088922	-2.657692	-0.122499
11	1	0	-2.932411	-3.734520	-0.150731
12	6	0	-4.430418	-2.189459	-0.146157
13	6	0	-4.646019	-0.788890	-0.108304
14	6	0	-3.575451	0.073844	-0.051366
15	1	0	0.719813	2.435213	0.087690
16	1	0	-5.660690	-0.400633	-0.124505
17	1	0	-3.781864	1.137264	-0.024225
18	14	0	-0.271209	-2.528151	0.001300
19	6	0	-0.035317	-3.629382	-1.518009
20	1	0	-0.088294	-3.037912	-2.439762
21	1	0	0.921898	-4.160604	-1.508100
22	1	0	-0.832189	-4.382659	-1.556201
23	6	0	-0.137964	-3.512155	1.614856
24	1	0	-0.293067	-2.855519	2.479029
25	1	0	-0.916302	-4.285424	1.636185
26	1	0	0.828738	-4.012054	1.737622
27	6	0	5.146018	-1.386677	0.056962
28	1	0	5.500866	-1.665564	-0.945527
29	1	0	6.031025	-1.230067	0.683760
30	7	0	-5.469257	-3.055027	-0.204249
31	1	0	-6.426392	-2.729717	-0.208408

32	6	0	4.670795	2.301164	-0.691975
33	1	0	4.432734	2.161442	-1.754053
34	1	0	5.359957	3.148593	-0.617053
35	6	0	3.389506	2.556961	0.103114
36	1	0	2.846914	3.425159	-0.285285
37	7	0	4.447672	-0.095714	-0.036674
38	6	0	5.359374	1.057819	-0.147195
39	1	0	3.652359	2.787378	1.146320
40	6	0	2.921757	-2.482382	-0.115613
41	1	0	3.107942	-2.732205	-1.170769
42	1	0	2.284068	-3.272376	0.283158
43	6	0	4.253759	-2.470881	0.635325
44	1	0	4.759575	-3.437556	0.544760
45	1	0	4.082123	-2.285874	1.703247
46	1	0	5.787876	1.254619	0.845954
47	1	0	6.183111	0.750798	-0.801030
48	6	0	-1.574895	2.031870	0.061247
49	6	0	-1.759785	2.738291	-1.148254
50	6	0	-1.796753	2.659496	1.307319
51	6	0	-2.167358	4.078506	-1.089711
52	6	0	-2.203686	4.001150	1.322475
53	6	0	-2.389213	4.709609	0.134829
54	1	0	-2.311178	4.628209	-2.016986
55	1	0	-2.375834	4.490506	2.278282
56	1	0	-2.705680	5.749188	0.163397
57	6	0	-1.524331	2.081630	-2.491053

58	1	0	-2.163438	1.201306	-2.630147
59	1	0	-1.735264	2.781366	-3.305280
60	1	0	-0.486675	1.743018	-2.599311
61	6	0	-1.600909	1.917889	2.611757
62	1	0	-2.241337	1.029762	2.673924
63	1	0	-0.566034	1.574070	2.730151
64	1	0	-1.838970	2.563464	3.462472
65	1	0	-5.323719	-4.055175	-0.217467

Ac-2,6-diMe JuloSiR (13)

LUMO -3.49 eV

HOMO -6.10 eV

E(RB3LYP) = -1676.58896006 a.u.

Center Number	Atomic Number	Atomic Type	Coordinates (Angstroms) X	Y	Z
1	6	0	3.481011	-1.048334	-0.022818
2	6	0	2.214576	-1.763197	-0.013753
3	6	0	1.009667	-1.085220	0.029993
4	6	0	0.992524	0.372013	0.045397
5	6	0	2.268544	1.037130	0.044943
6	6	0	3.469467	0.390900	0.024032
7	6	0	-0.164825	1.179084	0.046025
8	6	0	-1.551253	0.724273	0.017692

9	6	0	-1.924384	-0.648942	0.005445
10	6	0	-3.272834	-1.010150	-0.034621
11	1	0	-3.561705	-2.052618	-0.044890
12	6	0	-4.292806	-0.039263	-0.062328
13	6	0	-3.928229	1.320893	-0.044043
14	6	0	-2.596596	1.687437	-0.005275
15	1	0	2.286827	2.120559	0.067755
16	1	0	-4.696356	2.089868	-0.060895
17	1	0	-2.359413	2.744291	0.005811
18	14	0	-0.641809	-2.022841	0.070239
19	6	0	-0.892798	-3.142390	-1.432173
20	1	0	-0.707016	-2.593098	-2.362671
21	1	0	-0.238986	-4.020199	-1.416843
22	1	0	-1.929304	-3.501110	-1.455093
23	6	0	-0.887861	-2.952032	1.702025
24	1	0	-0.738818	-2.278719	2.554199
25	1	0	-1.915104	-3.334609	1.751138
26	1	0	-0.210977	-3.804768	1.819975
27	6	0	4.770365	-3.171355	0.013900
28	1	0	4.949616	-3.564551	-0.996272
29	1	0	5.663610	-3.382516	0.611000
30	7	0	-5.658735	-0.338430	-0.107838
31	1	0	-6.270150	0.469488	-0.130446
32	6	0	-6.291895	-1.564739	-0.135226
33	8	0	-5.685757	-2.635915	-0.111176
34	6	0	-7.803848	-1.504328	-0.208038

35	1	0	-8.218402	-2.118426	0.597281
36	1	0	-8.210838	-0.492981	-0.131463
37	1	0	-8.125716	-1.942658	-1.159020
38	6	0	5.825271	0.388434	-0.767488
39	1	0	5.532323	0.354532	-1.824284
40	1	0	6.801914	0.879668	-0.711140
41	6	0	4.776054	1.147571	0.045345
42	1	0	4.626124	2.159956	-0.342956
43	7	0	4.652650	-1.705671	-0.077363
44	6	0	5.955918	-1.024785	-0.219794
45	1	0	5.127956	1.252866	1.082206
46	6	0	2.291605	-3.275548	-0.087695
47	1	0	2.329302	-3.587652	-1.141787
48	1	0	1.399961	-3.733635	0.341672
49	6	0	3.534478	-3.798893	0.631884
50	1	0	3.604121	-4.887638	0.543817
51	1	0	3.483953	-3.555467	1.700511
52	1	0	6.443329	-1.020040	0.764791
53	1	0	6.564982	-1.648350	-0.882461
54	6	0	0.024902	2.676054	0.065928
55	6	0	0.118186	3.384298	-1.153069
56	6	0	0.086074	3.352486	1.304745
57	6	0	0.275682	4.776679	-1.110911
58	6	0	0.244309	4.745488	1.302747
59	6	0	0.338606	5.456520	0.105967
60	1	0	0.348480	5.328727	-2.044999

61	1	0	0.292595	5.273040	2.252434
62	1	0	0.459883	6.536625	0.121480
63	6	0	0.059599	2.672912	-2.487301
64	1	0	-0.859886	2.085210	-2.595625
65	1	0	0.096242	3.392878	-3.310238
66	1	0	0.899481	1.978311	-2.612386
67	6	0	-0.006773	2.606710	2.618091
68	1	0	-0.928633	2.016786	2.687223
69	1	0	0.829738	1.908680	2.746775
70	1	0	0.008436	3.305096	3.460111

2,6-diMe QuinoSiR (20)

LUMO -3.32 eV

HOMO -5.68 eV

E(RB3LYP) = -1563.21938811 a.u.

Center Number	Atomic Number	Atomic Type	Coordinates (Angstroms) X	Y	Z
1	6	0	-2.717737	-0.805496	0.002436
2	6	0	-1.632048	-1.737774	-0.007574
3	6	0	-0.305270	-1.354382	-0.013423
4	6	0	0.034462	0.044187	-0.009544
5	6	0	-1.058954	0.968581	-0.006138
6	6	0	-2.386176	0.596043	0.000176

7	6	0	1.371918	0.542579	-0.005108
8	6	0	2.582440	-0.235011	0.008183
9	6	0	2.617505	-1.674303	0.007364
10	6	0	3.833412	-2.334152	0.032673
11	1	0	3.865495	-3.422330	0.033503
12	6	0	5.075251	-1.640944	0.057806
13	6	0	5.046044	-0.223385	0.053018
14	6	0	3.842301	0.442015	0.028893
15	1	0	-1.863674	-2.795694	-0.011013
16	1	0	-0.832604	2.026591	-0.006552
17	1	0	5.978710	0.334005	0.069871
18	1	0	3.862256	1.525499	0.027540
19	14	0	1.029203	-2.683641	-0.041337
20	6	0	0.894349	-3.802042	1.472821
21	1	0	0.959016	-3.222956	2.401085
22	1	0	-0.060090	-4.342830	1.472990
23	1	0	1.699874	-4.546662	1.477273
24	6	0	0.926360	-3.685785	-1.638093
25	1	0	1.000037	-3.037310	-2.518618
26	1	0	1.738010	-4.422064	-1.686842
27	1	0	-0.024495	-4.230066	-1.692912
28	6	0	-4.278123	-2.672726	0.016920
29	1	0	-3.850066	-3.149208	0.904552
30	1	0	-5.351377	-2.838926	0.030339
31	1	0	-3.872026	-3.150159	-0.880505
32	7	0	6.245341	-2.316776	0.084576

33	1	0	7.133252	-1.833892	0.102616
34	6	0	-4.743891	1.130327	0.016418
35	1	0	-5.566690	1.841938	0.020716
36	6	0	-3.478134	1.576334	0.005705
37	7	0	-3.999358	-1.229721	0.013003
38	6	0	-5.181677	-0.311305	0.024232
39	6	0	-3.163817	3.051451	-0.000716
40	1	0	-2.572935	3.341284	0.877559
41	1	0	-2.583738	3.335743	-0.887965
42	1	0	-4.085578	3.640177	0.003175
43	6	0	-6.043496	-0.559686	-1.238835
44	1	0	-6.476673	-1.564466	-1.255440
45	1	0	-6.871714	0.156603	-1.257741
46	1	0	-5.444769	-0.418517	-2.144354
47	6	0	-6.015368	-0.554835	1.307029
48	1	0	-6.842203	0.162405	1.342259
49	1	0	-6.448940	-1.559192	1.336277
50	1	0	-5.396405	-0.411477	2.198465
51	6	0	1.537589	2.042150	-0.010086
52	6	0	1.609601	2.741071	1.215701
53	6	0	1.623202	2.728315	-1.242187
54	6	0	1.771047	4.133477	1.187352
55	6	0	1.784419	4.120958	-1.226553
56	6	0	1.858888	4.822511	-0.022771
57	1	0	1.828366	4.678049	2.126921
58	1	0	1.852186	4.655673	-2.171078

59	1	0	1.984569	5.902248	-0.027682
60	6	0	1.516850	2.020462	2.543086
61	1	0	2.316416	1.278653	2.658890
62	1	0	1.594405	2.729093	3.373032
63	1	0	0.565932	1.483915	2.647214
64	6	0	1.544539	1.994030	-2.562991
65	1	0	2.342694	1.248152	-2.660898
66	1	0	0.592950	1.459874	-2.673304
67	1	0	1.634997	2.693593	-3.399314
68	1	0	6.271168	-3.327275	0.090862

Ac-2,6-diMe QuinoSiR (21)

LUMO -3.58 eV

HOMO -6.00 eV

E(RB3LYP) = -1715.88424074 a.u.

Center Number	Atomic Number	Atomic Type	Coordinates (Angstroms) X	Y	Z
1	6	0	-3.078125	-1.276892	0.007948
2	6	0	-1.788362	-1.908260	-0.007064
3	6	0	-0.605065	-1.207188	-0.020111
4	6	0	-0.630168	0.239428	-0.013851
5	6	0	-1.927185	0.860386	-0.004060
6	6	0	-3.113920	0.168128	0.006257

7	6	0	0.525475	1.051241	-0.012366
8	6	0	1.911729	0.593510	-0.009255
9	6	0	2.301458	-0.780489	-0.020683
10	6	0	3.652949	-1.127729	-0.010476
11	1	0	3.950866	-2.167849	-0.019269
12	6	0	4.664960	-0.146645	0.011174
13	6	0	4.286401	1.209835	0.018651
14	6	0	2.951025	1.563881	0.008603
15	1	0	-1.749639	-2.990186	-0.009396
16	1	0	-1.971806	1.941306	-0.003271
17	1	0	5.046958	1.986248	0.033396
18	1	0	2.704358	2.618697	0.016083
19	14	0	1.023766	-2.158524	-0.061409
20	6	0	1.179497	-3.273933	1.451921
21	1	0	1.081851	-2.700171	2.380476
22	1	0	0.403545	-4.049167	1.444382
23	1	0	2.154215	-3.776906	1.461203
24	6	0	1.162719	-3.150019	-1.661142
25	1	0	1.062259	-2.502498	-2.539579
26	1	0	2.135195	-3.654376	-1.717106
27	1	0	0.382160	-3.918985	-1.710829
28	6	0	-4.111118	-3.478875	0.022852
29	1	0	-3.575616	-3.830302	0.909467
30	1	0	-5.108586	-3.907114	0.037983
31	1	0	-3.600860	-3.833853	-0.877224
32	7	0	6.032578	-0.433585	0.024161

33	1	0	6.637956	0.379357	0.040595
34	6	0	6.678355	-1.655342	0.039130
35	8	0	6.081522	-2.731028	0.020847
36	6	0	8.189217	-1.573235	0.110332
37	1	0	8.614298	-2.374518	-0.498951
38	1	0	8.589905	-0.612213	-0.223450
39	1	0	8.502758	-1.736374	1.148539
40	6	0	-5.527508	0.083507	0.029641
41	1	0	-6.504947	0.560516	0.037811
42	6	0	-4.418118	0.838530	0.016714
43	7	0	-4.202957	-2.009157	0.021359
44	6	0	-5.581662	-1.420729	0.034861
45	6	0	-4.488181	2.344567	0.012806
46	1	0	-3.987283	2.772786	0.890313
47	1	0	-4.002213	2.767389	-0.875658
48	1	0	-5.529045	2.679957	0.020619
49	6	0	-6.348763	-1.881688	-1.229608
50	1	0	-6.508816	-2.963759	-1.247153
51	1	0	-7.332924	-1.402358	-1.245890
52	1	0	-5.807366	-1.589352	-2.134794
53	6	0	-6.320477	-1.873855	1.318797
54	1	0	-7.303710	-1.393720	1.354241
55	1	0	-6.480646	-2.955712	1.346149
56	1	0	-5.758771	-1.576576	2.209897
57	6	0	0.321045	2.544721	-0.009218
58	6	0	0.226712	3.233019	1.221120

59	6	0	0.235138	3.236917	-1.237980
60	6	0	0.046090	4.623052	1.200285
61	6	0	0.054207	4.626865	-1.214006
62	6	0	-0.039567	5.318848	-0.006080
63	1	0	-0.026839	5.160377	2.142863
64	1	0	-0.012474	5.167134	-2.155367
65	1	0	-0.178869	6.396870	-0.004847
66	6	0	0.313021	2.503343	2.543910
67	1	0	1.252919	1.946547	2.640789
68	1	0	0.254235	3.208858	3.377945
69	1	0	-0.501779	1.778189	2.660431
70	6	0	0.330268	2.511364	-2.562445
71	1	0	1.271674	1.956466	-2.655555
72	1	0	-0.482597	1.785170	-2.685764
73	1	0	0.275099	3.219278	-3.394696

Supporting references:

[1] Y. Shimada, M. Imamura, T. Wagata, N. Yamaguchi, T. Tobe. *Cancer* **1992**, *69*, 277-284.

[2] A. D. Becke, *Phys. Rev. A* **1988**, *38*, 3098–3100.

[3] A. D. Becke, *J. Chem. Phys.* **1993**, *98*, 1372–1377.

[4] A. D. Becke, *J. Chem. Phys.* **1993**, *98*, 5648–5652.

[5] C. Lee, W. Yang, R. G. Parr, *Phys. Rev. B.* **1988**, *37*, 785–789.

[6] Gaussian 09, Revision A.02, M. J. Frisch, G. W. Trucks, H. B. Schlegel, G. E. Scuseria, M. A. Robb, J. R. Cheeseman, G. Scalmani, V. Barone, G. A. Petersson, H. Nakatsuji, X. Li, M. Caricato, A. Marenich, J. Bloino, B. G. Janesko, R. Gomperts, B. Mennucci, H. P. Hratchian, J. V. Ortiz, A. F. Izmaylov, J. L. Sonnenberg, D. Williams-Young, F. Ding, F. Lipparini, F. Egidi, J. Goings, B. Peng, A. Petrone, T. Henderson, D. Ranasinghe, V. G. Zakrzewski, J. Gao, N. Rega, G. Zheng, W. Liang, M. Hada, M. Ehara, K. Toyota, R. Fukuda, J. Hasegawa, M. Ishida, T. Nakajima, Y. Honda, O. Kitao, H. Nakai, T. Vreven, K. Throssell, J. A. Montgomery, Jr., J. E. Peralta, F. Ogliaro, M. Bearpark, J. J. Heyd, E. Brothers, K. N. Kudin, V. N. Staroverov, T. Keith, R. Kobayashi, J. Normand, K. Raghavachari, A. Rendell, J. C. Burant, S. S. Iyengar, J. Tomasi, M. Cossi, J. M. Millam, M. Klene, C. Adamo, R. Cammi, J. W. Ochterski, R. L. Martin, K. Morokuma, O. Farkas, J. B. Foresman, and D. J. Fox, Gaussian, Inc., Wallingford CT, 2016.

[7] Y. Koide, Y. Urano, K. Hanaoka, W. Piao, M. Kusakabe, N. Saito, T. Terai, T. Okabe, T. Nagano, *J. Am. Chem. Soc.* **2012**, *134*, 5029–5031.

[8] T. Egawa, Y. Koide, K. Hanaoka, T. Komatsu, T. Terai, T. Nagano, *Chem. Commun.* **2011**, *47*, 4162–4164.

[9] K. Hanaoka, Y. Kagami, W. Piao, T. Myochin, K. Numasawa, Y. Kuriki, T. Ikeno, T. Ueno, T. Komatsu, T. Terai, T. Nagano, Y. Urano, *Chem. Commun* **2018**, *54*, 6939-6942.

[10] R. J. Iwatate, M. Kamiya, K. Umezawa, H. Kashima, M. Nakadate, R. Kojima, Y. Urano, *Bioconjug. Chem.* **2018**, *29*, 241–244.

[11] C. Reichardt, *Chem. Rev.* **1994**, *94*, 2319-2358.

[12] P. Puppan, *J. Photochem. Photobiol. A* **1990**, *50*, 293-330.

[13] H. Lu, S. C. Rutan, *Anal. Chem.* **1996**, *68*, 1381-1386.